WESTINGHOUSE PROPRIETARY CLASS 3

WCAP-10252

SECOND CYCLE PERFORMANCE OF BEAVER VALLEY UNIT 1 FUEL

By

P. A. Pritchett

H. Kunishi

Approved: E Roberts

E. Roberts, Manager
Irradiation Testing

Westinghouse Electric Corporation
Nuclear Energy Systems
P. O. Box 355
Pittsburgh, Pennsylvania 15230

Table of Contents

List of Illustrations

List of Illustrations (continued)

List of Tables

1.0 INTRODUCTION

The 17x17 fuel assembly is in extensive operation in recent Westinghouse 3-loop and 4-loop reactors with power up to 3800 MWT and average linear power of 5.4 kw/ft. This design extends fuel capability beyond that of the 15x15 design in use to date in reactors of this size. It was adopted primarily in response to the lowered average kw/ft requirements imposed by the AEC Interim Acceptance Criteria. While the primary intent of the design is to reduce stored energy in fuel rods for LOCA conditions, it is also expected that rod bow will be decreased because of the shorter grid span lengths characteristic of the 17x17 design.

The NRC has required fuel surveillance inspections on the first several 17x17 plants to go into operation, including Beaver Valley Unit 1, to verify satisfactory fuel performance.

The purpose of the Beaver Valley fuel examination was to evaluate the mechanical integrity of fuel rods and fuel assembly structural components, fuel surface condition, rod-to-nozzle gap and fuel rod bow; and to compare the Beaver Valley fuel performance with that of other 17x17 fuels.

Beaver Valley completed cycle 1 in November, 1979. Thirty-five fuel assemblies were non-destructively examined with underwater television and a large number of assemblies were binocular examined. The visual examination showed the assemblies to be in excellent mechanical condition.(1)

Cycle 2 of Beaver Valley Unit 1 was completed in December, 1981. One hundred fifty-three (153) fuel assemblies were binocular examined and thirty (30) fuel assemblies were T.V. visually examined with underwater television consistent with the planned program. Of the thirty fuel assemblies, ten fuel assemblies were selected as representative fuel assemblies from Regions 2 and 3 and the remaining twenty fuel assemblies were examined for possible effects of coolant cross flow through baffle joints. In addition, several assemblies, supplementary to the planned program were examined due to fuel handling problems.

2.0 BEAVER VALLEY UNIT 1 FUEL DESIGN

Duquesne Light, Beaver Valley Unit 1 is a 3-loop 17x17 reactor with 2652 MW thermal power rating. The fuel in Beaver Valley Unit 1 is of the low parasitic design. Each of the 157 fuel assemblies in the reactor core contains 264 Zircaloy-4 clad fuel rods. Each rod is approximately thirteen feet long and contains a twelve-foot long column of fuel pellets. Spacing between the fuel rods is maintained by eight Inconel 718 alloy grids nearly equally spaced along the length of the fuel rods. In each fuel assembly, the top and bottom nozzles and the eight grids are attached to twenty-four Zircaloy-4 thimble tubes which extend between the nozzles and through the eight grids. In the Region 4 fuel, pellet density was 95 percent of theoretical density, and the fuel rods were prepressurized with helium to [ ] psig. In Table 2-1, several Beaver Valley Unit 1 core design and operating characteristics are compared with those of Salem Unit 1 (Public Service Electric and Gas Co.), Salem Unit 2 (Public Service Electric and Gas Co.), and Trojan (Portland General Electric Company) reactors. (a,c)

While physical dimensions of the Beaver Valley Unit 1 fuel are the same as in the standard 17x17 design in the Salem Unit 1, Salem Unit 2 and Trojan reactors the nuclear and thermal characteristics are not identical. Core average linear power is lower in Beaver Valley than Trojan and both Salem Units.

TABLE 2-1

CORE DESIGN AND OPERATING CHARACTERISTICS

UO_2 Enrichment w/o U-235	(a,c)
Region 1	
Region 2	
Region 3	
Region 4	
Coolant Temperature	
Hot Zero Power, °F	
Initial Inlet	
Initial Core Ave. HFP, °F	
Operating Coolant Pressure, psig	
Average Linear Power kw/ft	

3.0 BEAVER VALLEY UNIT 1 SECOND CYCLE OPERATING HISTORY

Beaver Valley Unit 1 achieved criticality in the second cycle in November, 1980 and completed the second cycle in December, 1981 with Cycle 2 average burnup of 9,640 MWD/MTU. A brief summary of region burnup and powers is given in Table 3-1.[2]

Reactor power history and temperature history are plotted in figures 3-1 and 3-2. The Cycle 2 core loading pattern is shown in figure 3-3.

The activity of the fission products I-131 and I-133 in the primary coolant was measured during Cycle 2 to monitor the defect condition of the fuel. Iodine activity is an important indicator of fuel integrity. Although there is no quantitative correlation of activity with the number of fuel rod defects, because large defects release more activity than small defects and because reactor power transients cause sudden transient activity increases or spikes, activity levels in a general sense reflect the condition of the fuel. The I-131/I-133 activity ratio is an indicator of the type of defect. A low I-131/I-133, ratio results from an open fuel rod defect, one which allows rapid release into the coolant of both the longer half life I-131 and the shorter half life I-133. A closed defect restricts release of iodine from the fuel rod and since the short-lived I-133 decays to its daughter Xe 133 more rapidly than does the I-131 the ratio of I-131 to I-133 in the coolant is higher. A ratio of 0.1 to 0.3 indicates rapid release through an open defect and a ratio greater 0.5 indicates delay of iodine release through a tight defect. Figure 3-4 shows the activity in the coolant during Cycle 2. All iodine measurements reported here were made at or near full power thus avoiding transients or spikes associated with increasing or decreasing power. At the beginning of Cycle 2, iodine activity was similar to that at the end of Cycle 1. During Cycle 2, the activity remained constant until near the end of Cycle 2 where a small increase in the iodine levels appears to have occurred. Some scatter in the data exists, however, the I-131/I-133 activity ratio also appears to have decreased late in the cycle, indicating the possibility of an open

type defect. The coolant iodine activity remained less than 5 percent of the technical specification limit (1μ Ci/ml of I-131) for most of the Cycle 2, typcial of a low-defect core.

Figure 3-5 shows boron-lithium concentration for Cycles 1 and 2. Beaver Valley operated in a crud dissolving mode for both cycles. The critical solubility curve of figure 3-5 represents the dividing line between crud precipitating and crud dissolution based on the crud transportation processes developed by Westinghouse.(3) Below the solubility curve, there is a tendency for magnetite precipitation on hotter surfaces, assuming a saturated solution. Above the curve, the solubility of magnetite increases with temperature, thus there should be a tendency to dissolve the material from the core surface, or at least retard the precipitation.(4)

TABLE 3-1

POWER AND BURNUP HISTORY SUMMARY FOR BEAVER VALLEY UNIT 1

Region	Cycle 1 Average Power kw/ft)	Cycle 1 Burnup (MWD/MTU)	Cycle 2 Average Power (kw/ft)	Cycle 2 Burnup (MWD/MTU)	
1					(a,c)
2					
3					
4					
4A					

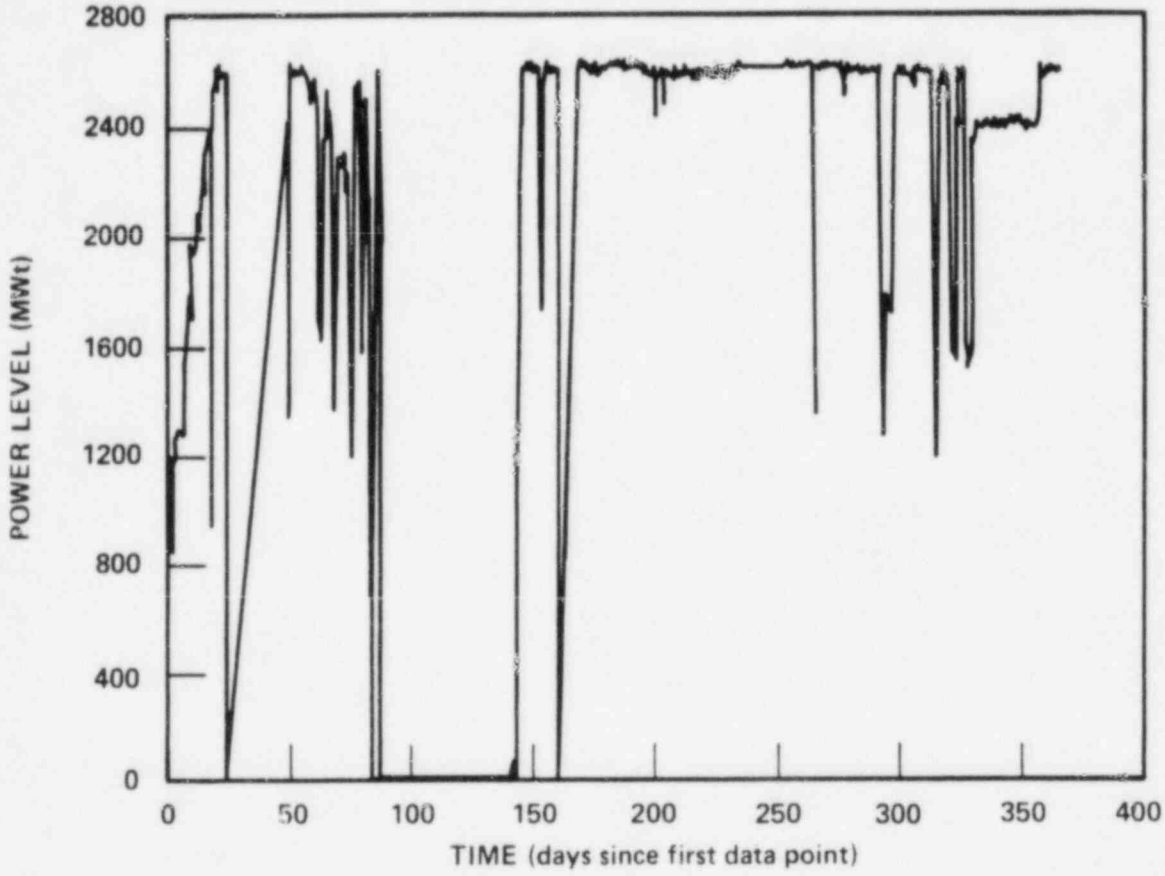

Figure 3-1. Cycle 2 Power History

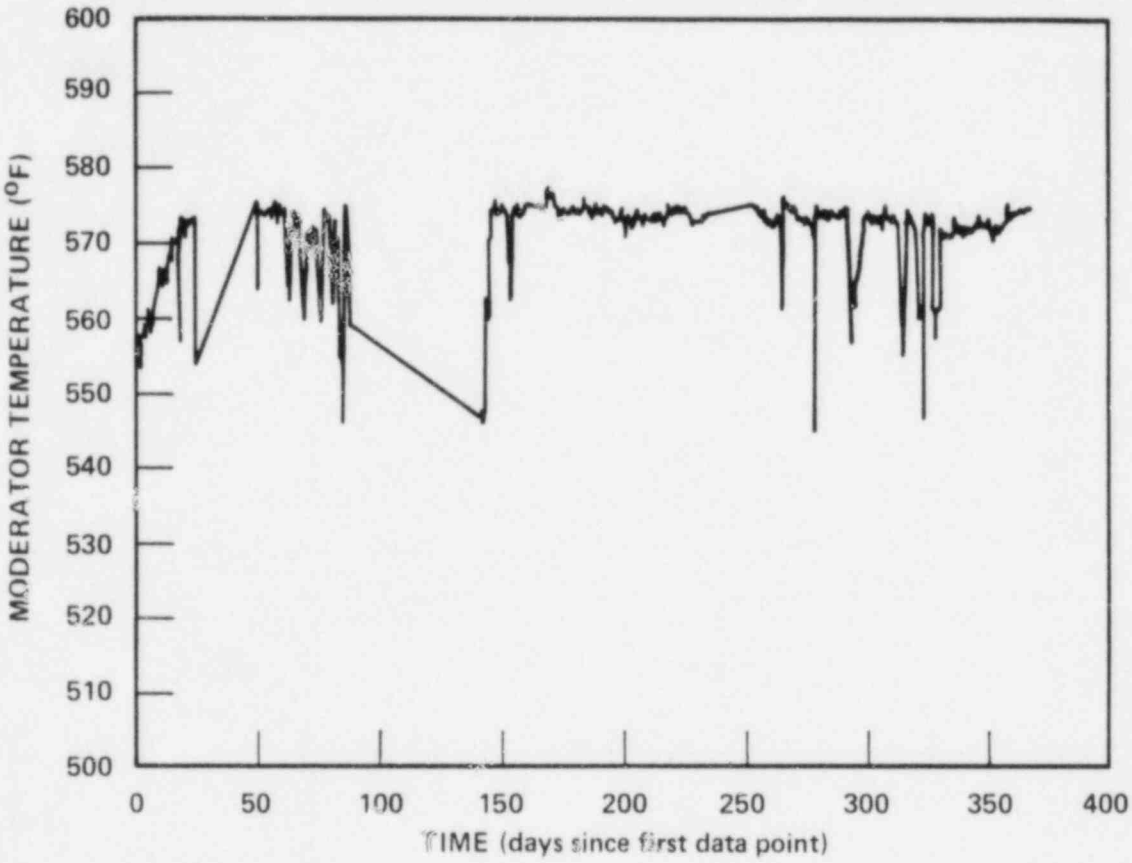

Figure 3-2. Cycle 2 Moderator Temperature History

2485-1

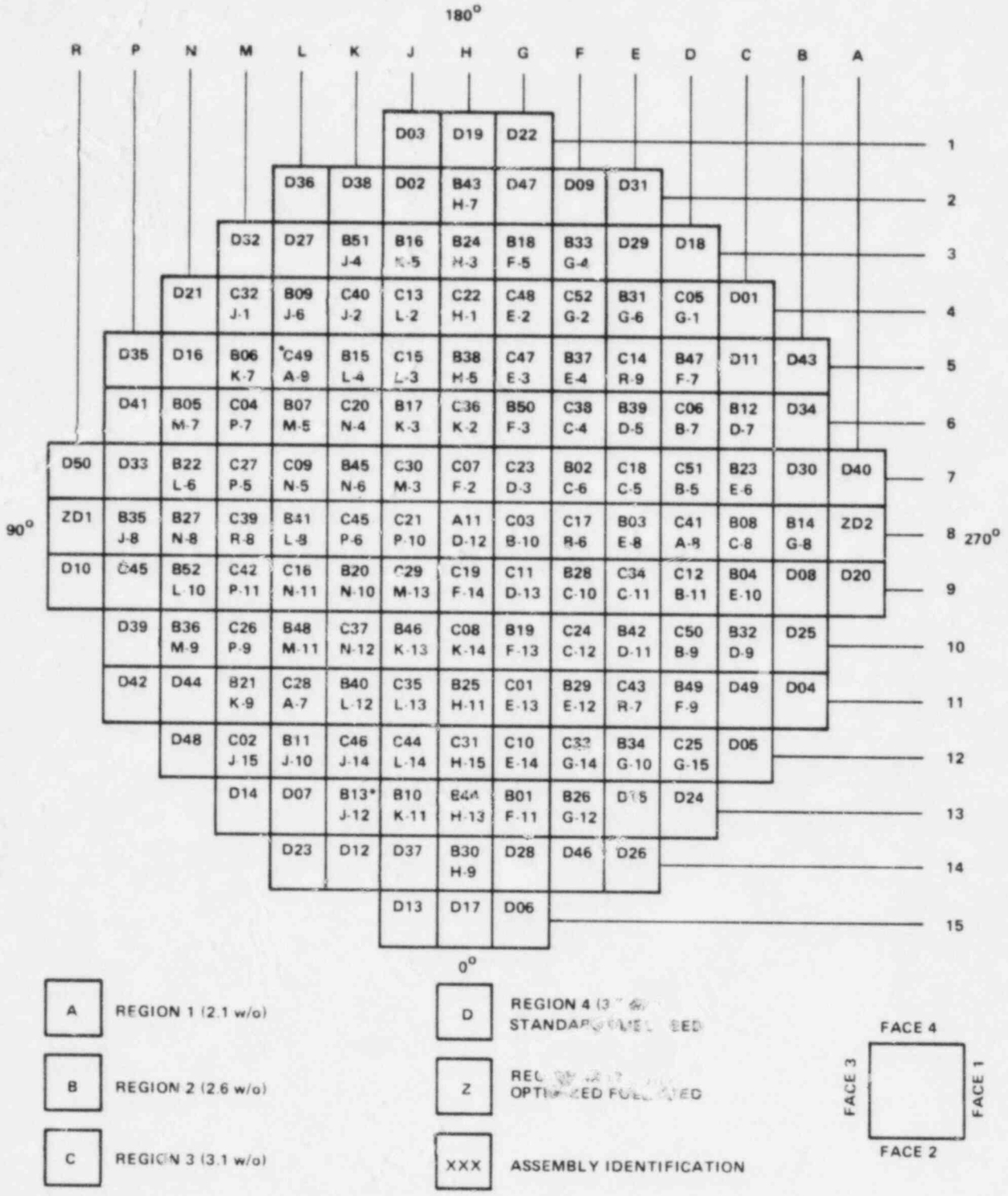

Figure 3-3. Cycle 2 Core Loading Pattern

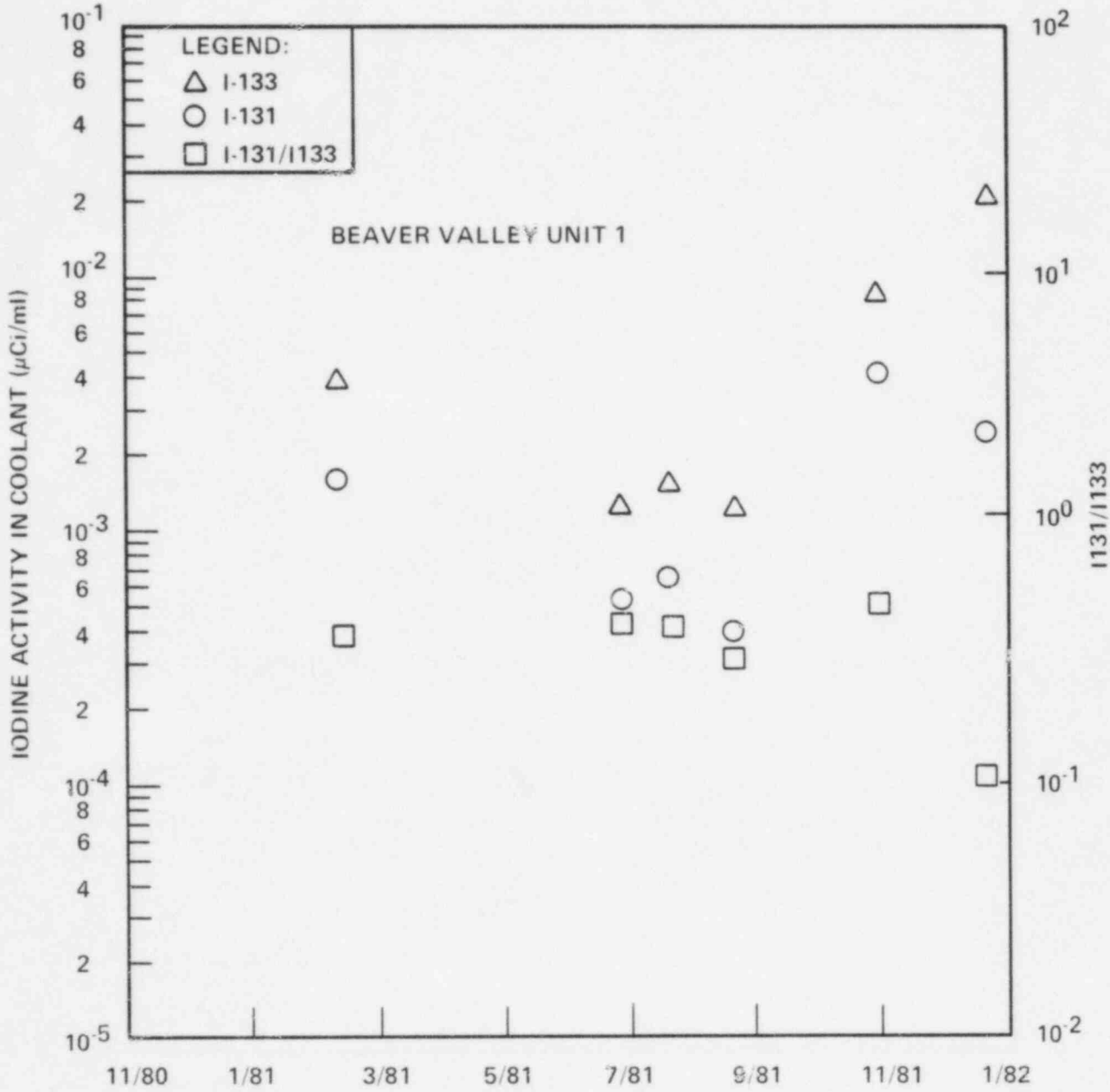

Figure 3-4. Cycle 2 Coolant Activity

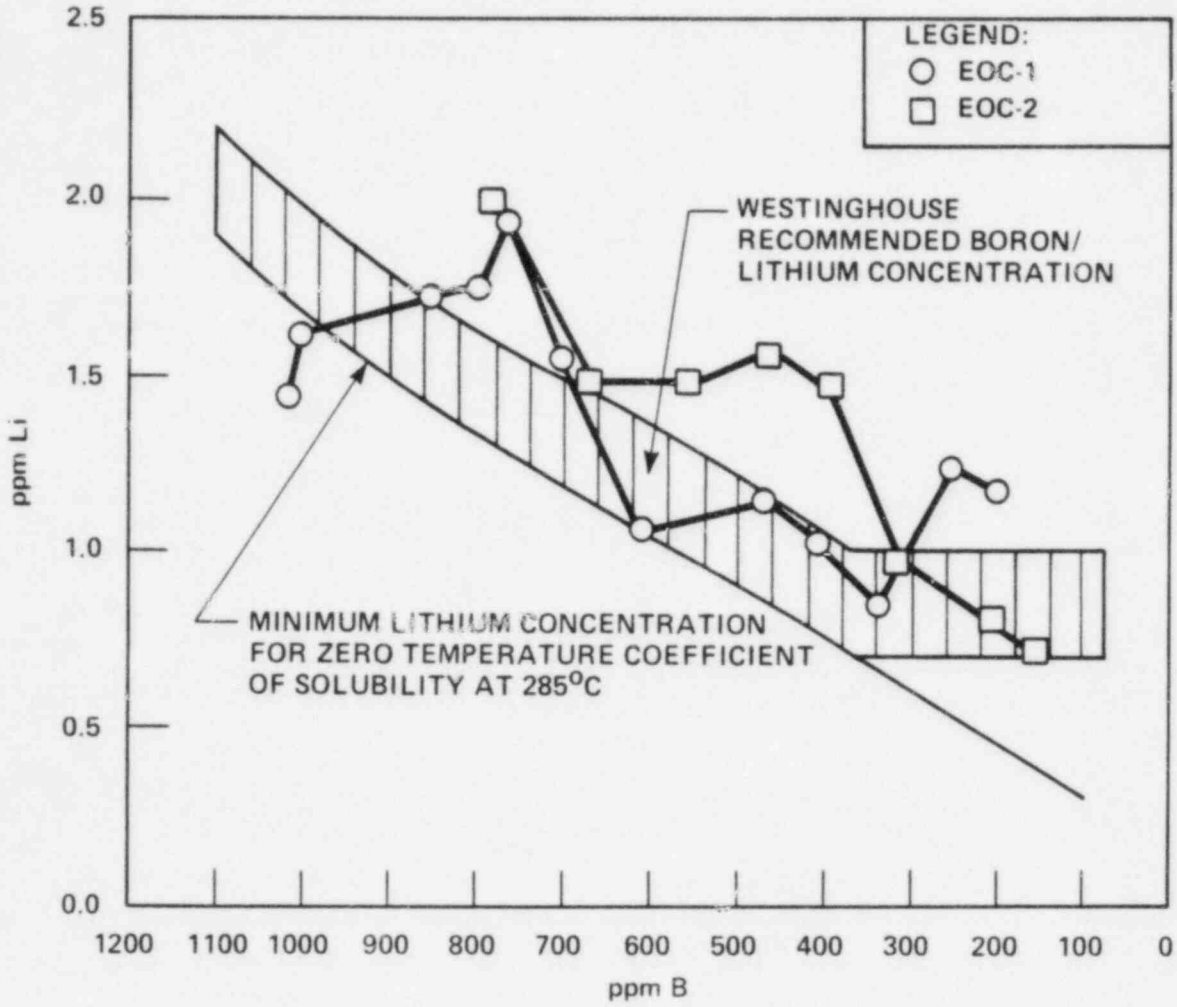

Figure 3-5. Boron Versus Lithium Concentration in DLW's Reactor Coolant During Cycle 1 and Cycle 2

4.0 FUEL EXAMINATION

At the end of cycle 2, Duquesne Light Company and Westinghouse conducted a planned, non-destructive visual examinations, one hundred fifty-three assemblies were examined by binocular to assess the overall integrity (the assemblies are listed in Table 4-1); ten (10) fuel assemblies from Regions 2 and 3 were examined by T.V. visuals to assess fuel assembly and fuel rod mechanical integrity, distribution of crud deposits, corrosion of fuel rod surfaces, and fuel rod bow (the assemblies examined are listed in Table 4-2); twenty Region 4 fuel assemblies located adjacent to the core baffle were examined by T.V. visuals for effects of possible coolant cross flow through baffle joints (the assemblies are listed in Table 4-6).

In addition, several fuel assemblies, supplementary to the planned program were examined. The fuel assemblies examined and the reason for the examination are given in Table 4-3.

4.1 BINOCULAR EXAMINATION

As fuel assemblies were transferred from the upender to the fuel storage rack in the spent fuel pool, 153 were viewed from above water at the side of the pool with 7X binoculars, to assess the overall condition. Examinations were performed on one (1) Region 1 assembly, 50 (fifty) Region 2 assemblies, 49 (forty-nine) Region 3 assemblies, 47 (forty-seven Region 4 assemblies and 6 (six) Region 5 assemblies (new assemblies).

Each assembly was examined as it was rotated about its longitudinal axis before it was inserted into the storage rack. The binocular examination did not reveal any anomalies such as failed rods, damaged grids, unusual conditions of rod bow, or unusual crud distribution or corrosion on peripheral fuel rods which could require a more detailed examination with underwater television.

TABLE 4-1

BEAVER VALLEY EOC-2 BINOCULAR EXAMINATION OF ASSEMBLIES

Region 1	Region 2	Region 3	Region 4	Region 5
All	B01	C01	ZD1	E14
	B02	C02	ZD2	E36
	B03	C03	D01	E10
	B04	C05	D02	E40
	B05	C06	D03	E46
	B07	C07	D04	E44
	B08	C08	D05	
	B09	C09	D06	
	B10	C10	D07	
	B11	C11	D08	
	B12	C12	D09	
	B13	C13	D11	
	B14	C14	D12	
	B15	C15	D13	
	B16	C16	D14	
	B17	C17	D15	
	B18	C18	D16	
	B19	C19	D17	
	B20	C21	D18	
	B21	C22	D19	
	B22	C23	D20	
	B23	C24	D21	
	B24	C25	D22	
	B25	C26	D23	
	B26	C27	D24	
	B27	C28	D25	
	B28	C29	D26	
	B29	C31	D27	
	B30	C32	D28	
	B31	C33	D29	
	B32	C34	D31	
	B33	C35	D32	
	B34	C36	D33	
	B35	C37	D34	
	B36	C38	D35	
	B37	C39	D36	
	B38	C40	D38	
	B39	C41	D39	
	B40	C42	D40	
	B41	C43	D41	
	B42	C44	D43	
	B43	C45	D44	
	B44	C46	D45	
	B45	C47	D46	
	B46	C48	D47	
	B47	C49	D48	
	B48	C50	D49	
	B49	C51		
	B51	C52		
	B52			

TABLE 4-2

BEAVER VALLEY UNIT 1 PLANNED EOC-2 T.V. VISUAL EXAMINATION

Fuel Assembly No.	Core Location	Comment
B04	C09	Examined at EOC-1
B07	L06	Examined at EOC-1
B13	K13	Examined at EOC-1
B20	K09	Examined at EOC-1
B31	E04	Examined at EOC-1
C03	G08	Examined at EOC-1
C06	D06	Examined at EOC-1
C15	J05	Examined at EOC-1
C39	M08	Examined at EOC-1
C49	L05	Examined at EOC-1

TABLE 4-3

BEAVER VALLEY UNIT 1 UNPLANNED EOC-2 EXAMINATION

Fuel Assembly No.	Core Location (Cycle 2)	Comment
C40	K04	Prematurely lowered in upender
C10	G12	Tilt in the core during reload
D17	H15	Adjacent to C10
C52	F04	Suspected to be bowed and twisted and suspected to cause C10 to tilt

4.2 TELEVISION EXAMINATION - GENERAL FUEL CONDITION

The low magnification television examination was a full face examination of all fuel assembly faces from the bottom nozzle to the top nozzle. Each fuel assembly was positioned in front of the television camera so that the field of view covered an area 3 x 4 inches of the assembly face. The assembly was lowered or raised in front of the television camera, scanning from nozzle to nozzle. The left half of the assembly face was examined in the first scan, and the right half of the face was examined in the second scan. Routinely, each scan was halted, briefly, at the bottom and top nozzles at each grid and at each mid-span position between grids.

T.V. tapes of the 10 (ten) fuel assemblies, which were also T.V. visually examined at the EOC-1, 5 (five) from Region 2 and 5 (five) from Region 3 were reviewed to assess general fuel assembly mechanical conditions. All fuel assemblies were in good mechanical condition. None of the fuel rods, top and bottom nozzles, grids, or hold-down springs were damaged.

T.V. tapes of the 4 (four) fuel assemblies examined supplementary were also reviewed to identify the possible anomaly. Assembly C40 which was prematurely lowered in the upender before it was completely positioned in the upender and released from the fuel assembly handling tool, showed no damage. Assembly C10, which tilted in the core during the core reload contacting with the north baffle wall showed no apparent damage; only minor scratches were observed on the assembly. Assembly D17 which was adjacent to C10 showed no damage. Assembly C52, suspected as being bowed and twisted and suspected to cause C10 to tilt showed no unusual conditions.

4.2.1 FUEL ROD SURFACE CONDITION

The T.V. tapes of ten representative fuel assemblies from Regions 2 and 3 were reviewed to examine corrosion patterns and crud distribution on fuel rods. No unusual crud deposits or cladding corrosion patterns was observed.

Fuel rods for Regions 2 and 3 exhibited the same general appearance. The fuel rod surfaces at the EOC-2 were generally similar to the EOC-1 observations with the additional deposition of crud during cycle 2. Figure 4-1 illustrates the comparison between EOC-1 and EOC-2 fuel rod surface appearance at corresponding elevation for assembly C49. The fuel rod surface from spans 1 through span 4 exhibited a mottle appearance similar to span 3 at the EOC-1. Spans 5 through 7 showed a relatively dark non-reflective and uniformly distributed crud.

The comparison between the EOC-1 and EOC-2 distribution suggests that the crud build up in cycle 2 is less than that in cycle 1. Less crud deposition in the observed cycle 2 is attributed to the high lithium concentration in cycle 2 as mentioned in Section 3.

4.2.2 PERIPHERAL FUEL ROD CHANNEL CLOSURE

Ten representative fuel assemblies from Regions 2 and 3 were evaluated to determine the peripheral rod channel closure with a low magnification T.V. Instead of measuring the data for every channel, only channel closures greater than [ ] percent were measured. Each closure was (a,c)
calculated from the expression

$$\text{CLOSURE} = \left[1 - \frac{M}{\frac{T+B}{2}}\right] \times 100 \quad \text{where}$$

M = spacing between two adjacent fuel rods at mid-span location between grids

T = spacing between two adjacent fuel rods at the top of the grid span

B = spacing between two adjacent fuel rods at the bottom of the grid span

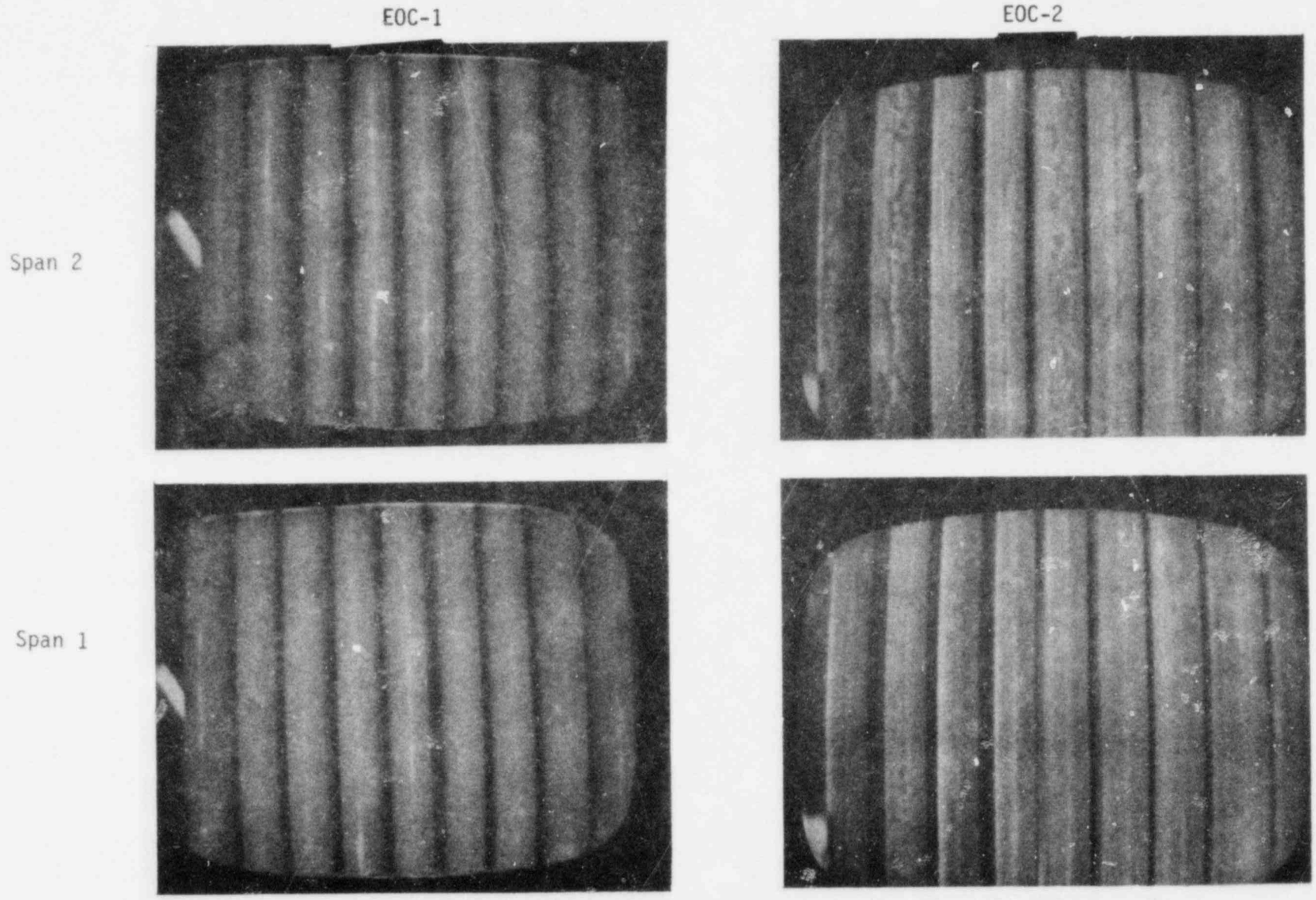

Figure 4-1 Surface Condition of Peripheral Fuel Rods in Beaver Valley Fuel Assembly C49 Face 3 Left Side EOC-1 and EOC-2 (Sheet 1 of 4)

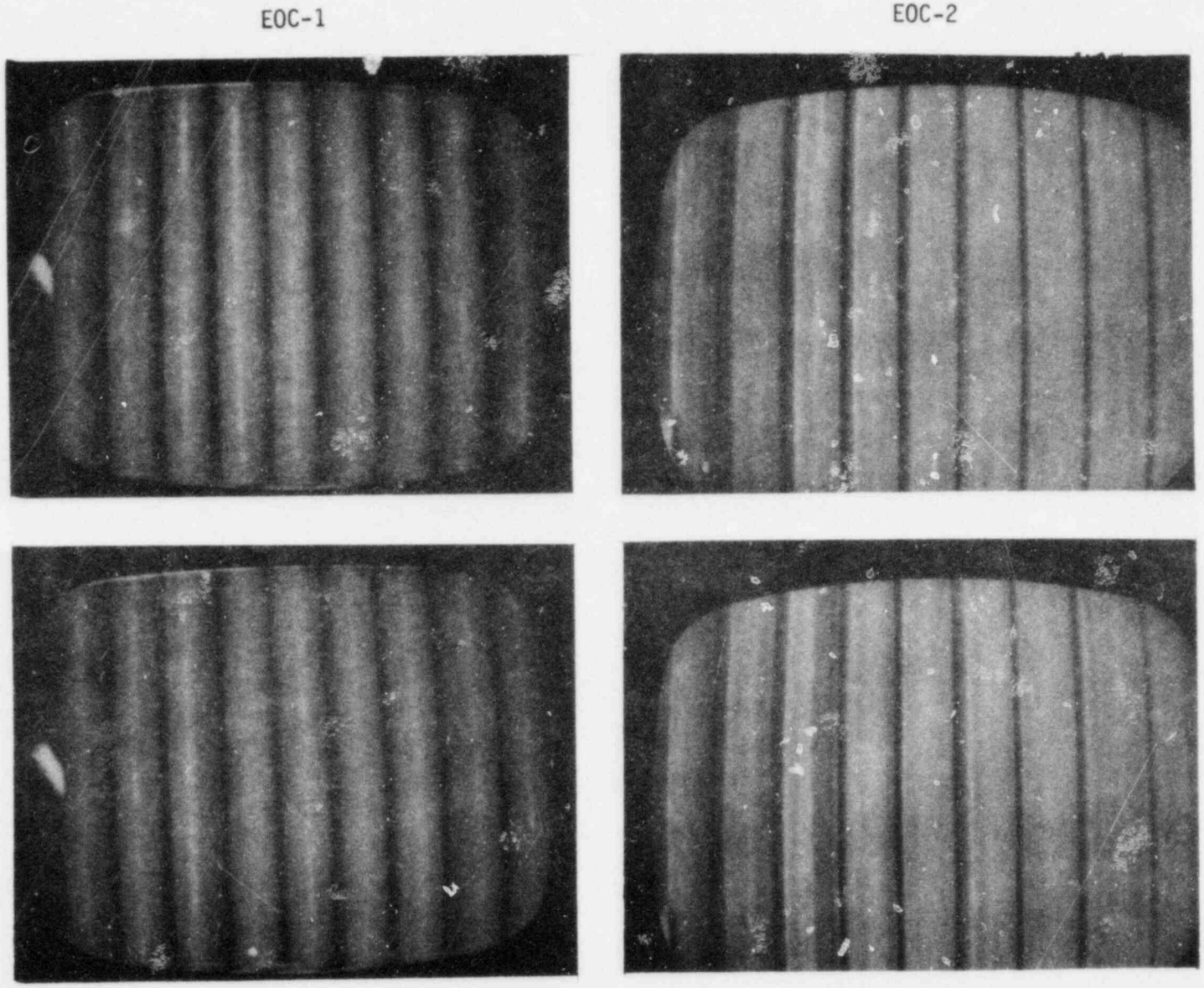

Figure 4-1 Surface Condition of Peripheral Fuel Rods in Beaver Valley Fuel Assembly C49 Face 3 Left Side EOC-1 and EOC-2 (Sheet 2 of 4)

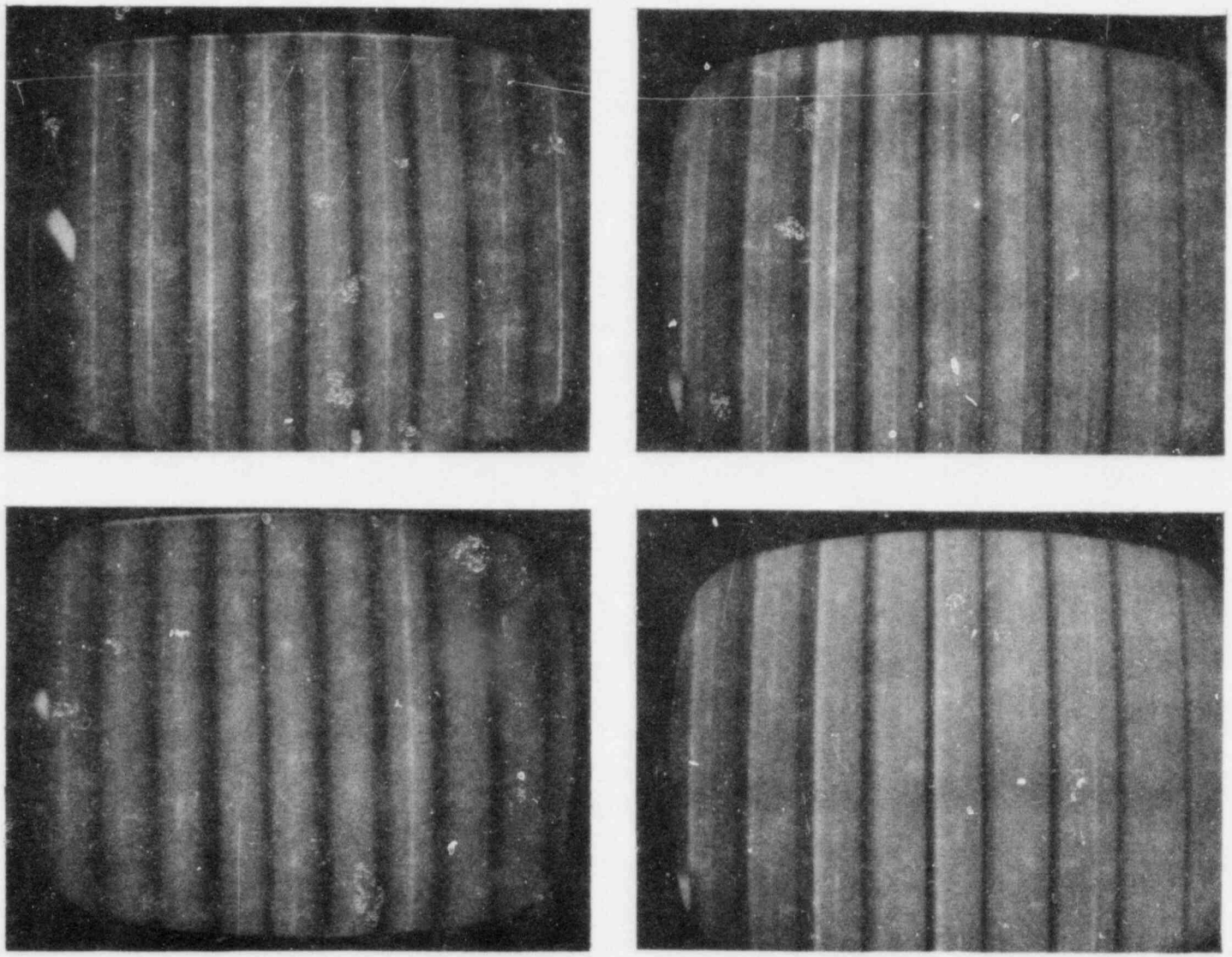

Figure 4-1 Surface Condition of Peripheral Fuel Rods in Beaver Valley Fuel Assembly C49 Face 3 Left Side EOC-1 and EOC-2 (Sheet 3 of 4)

EOC-1

EOC-2

Span 7

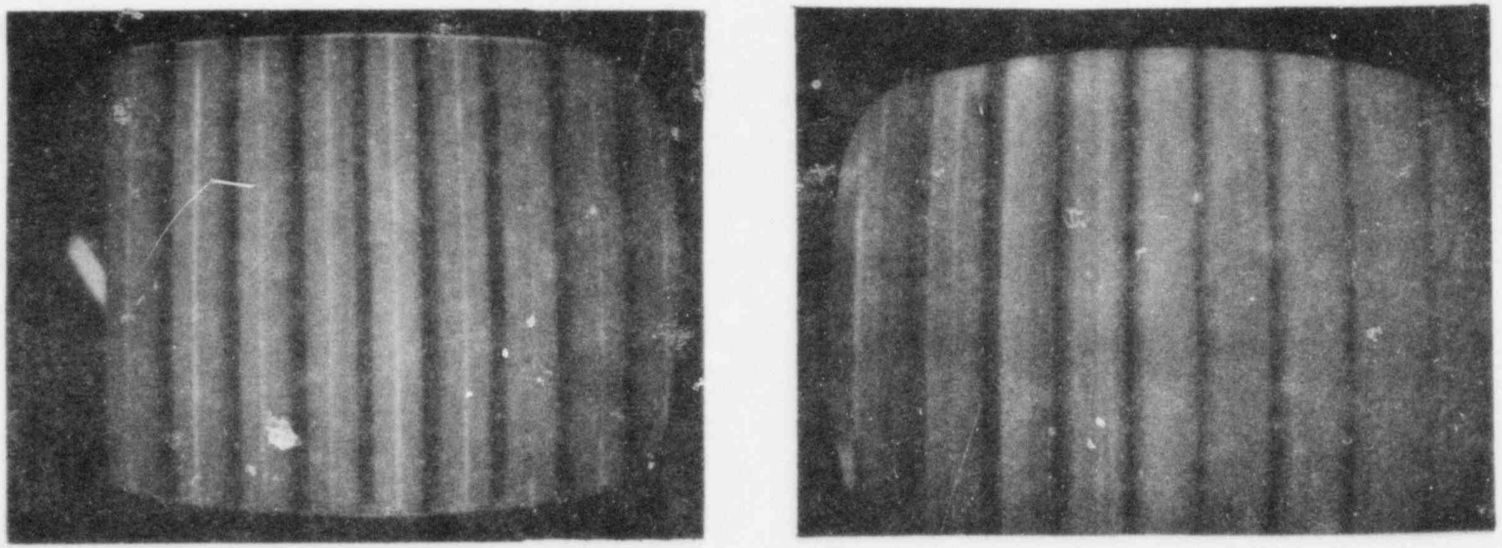

Figure 4-1 Surface Condition of Peripheral Fuel Rods in Beaver Valley Fuel Assembly C49 Face 3 Left Side EOC-1 and EOC-2 (Sheet 4 of 4)

The largest closure observed at EOC-2 was [ ] percent, the channel between rods 10 and 11, span 4, face 4 of Region 2 fuel assembly B13. The closure is shown in figure 4-2. This channel was [ ] percent closed at EOC-1. Only [ ] of the 10880 peripheral channels examined were closed [ ] percent or more. Table 4-4 lists all channels with greater than [ ] percent closure. A summary of the closure for each assembly is given in the Appendix A. (b,c)

The axial variation of channel closure in each region is shown in figure 4-3. The span 1 closure in figure 4-3 has been normalized to compensate for the longer length of the first span (24 inches in span 1 and 20 inches in the upper span). The closure in span 1 was normalized by the ratio $\left(\frac{20}{24}\right)^2$. (This is derived from ratio of flexural rigidity $(I/1)^2$ between 24-inch-span and 20-inch-span). The worst span closure occurred in span 4 for Region 2 assemblies and span 2 for the Region 3 assemblies as can be seen in figure 4-3. The occurrence of worst-span closure in the bottom half of the fuel assembly was also observed in previous examination of Trojan 8-grid 17 x 17 fuel[6], Salem 8-grid, 17x17 fuel[5] and the Surry 7-grid, 17x17 demonstration fuel assemblies[7,8]. In figure 4-4, the 95th - percentile closure in the worst-axial grid span of Beaver Valley at EOC-1 and EOC-2 as well as Surry 7-grid 17x17 assemblies, Trojan 8-grid 17x17 assemblies and Salem 8-grid 17x17 assemblies are shown. The rod bow design limit curve approved by the NRC is also shown. The Surry data (7-grid) have been normalized to the same length as the 8 grid standard 17x17 fuel in other reactors. As seen in figure 4-4, Beaver Valley closures are well below the design curve for the 8 grid 17x17 design and consistent with other data.

4.2.3 PERIPHERAL FUEL ROD-TO-NOZZLE GAP AND ROD GROWTH

The axial gap between peripheral fuel rod and assembly nozzle for nine assemblies, B04, B07, B13, B20, B31, C03, C06, C15 and C39 was measured from the low magnification image on the television monitor.

TABLE 4-4

FUEL ROD CHANNEL CLOSURES [ ] PERCENT
IN BEAVER VALLEY UNIT 1 FUEL AT EOC-2

Assembly	Face	Span	Rod	EOC-1	EOC-2	
B07						(b,c)
B13						
B31						
C15						
C39						
C49						

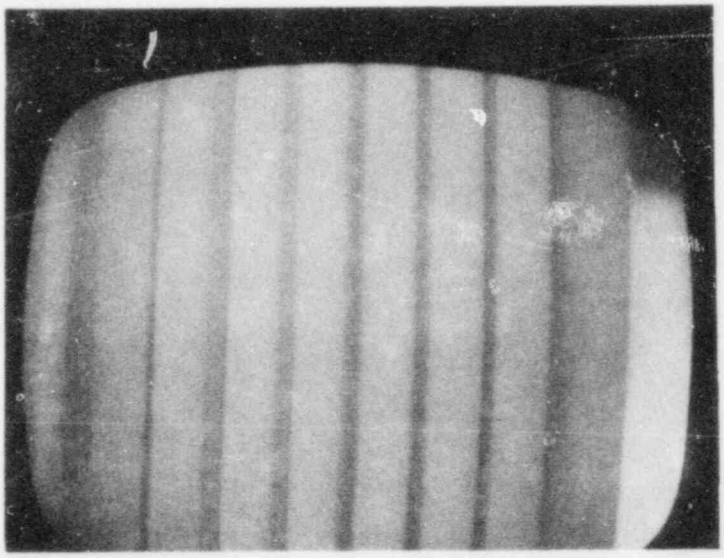

Figure 4-2 Maximum Channel Closure ( ) Percent Assembly B13, Face 4 Span 4 between Rods 10 and 11 (b,c)

3760

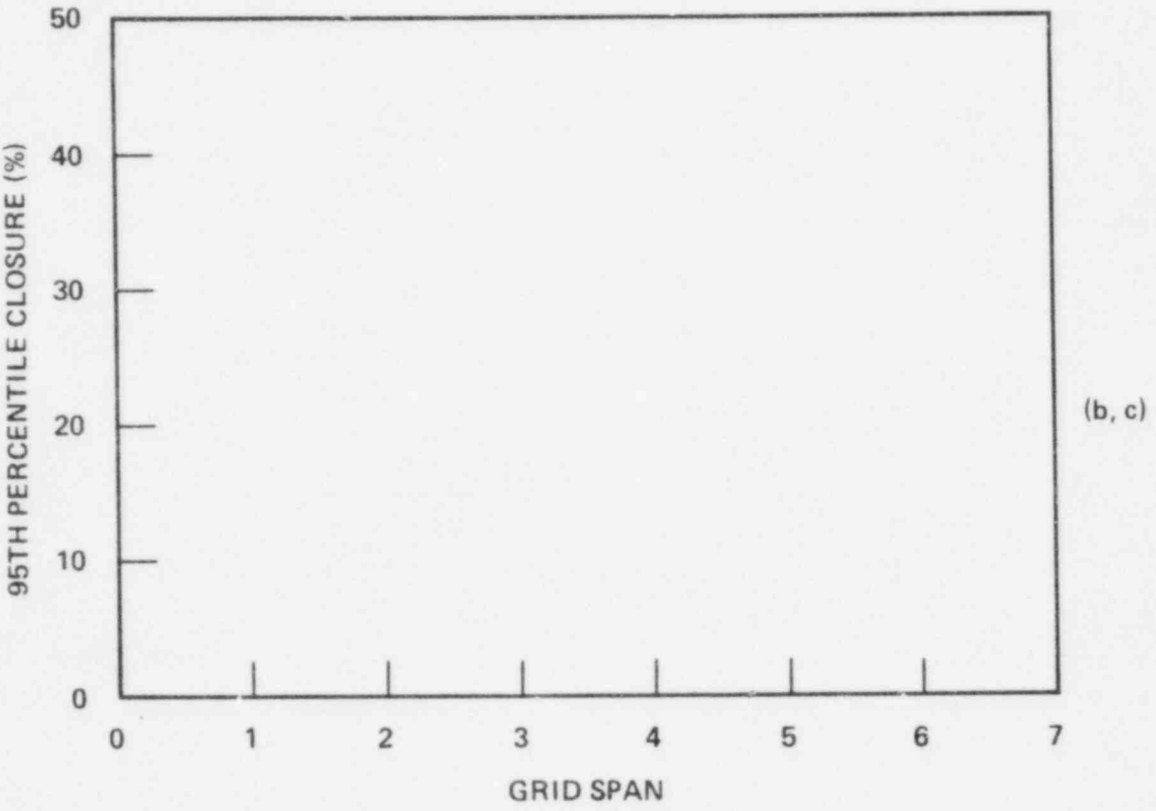

Figure 4-3. EOC-2 Axial Variation in 95th Percentile Peripheral Fuel Rod Channel Closure in Beaver Valley Unit 1

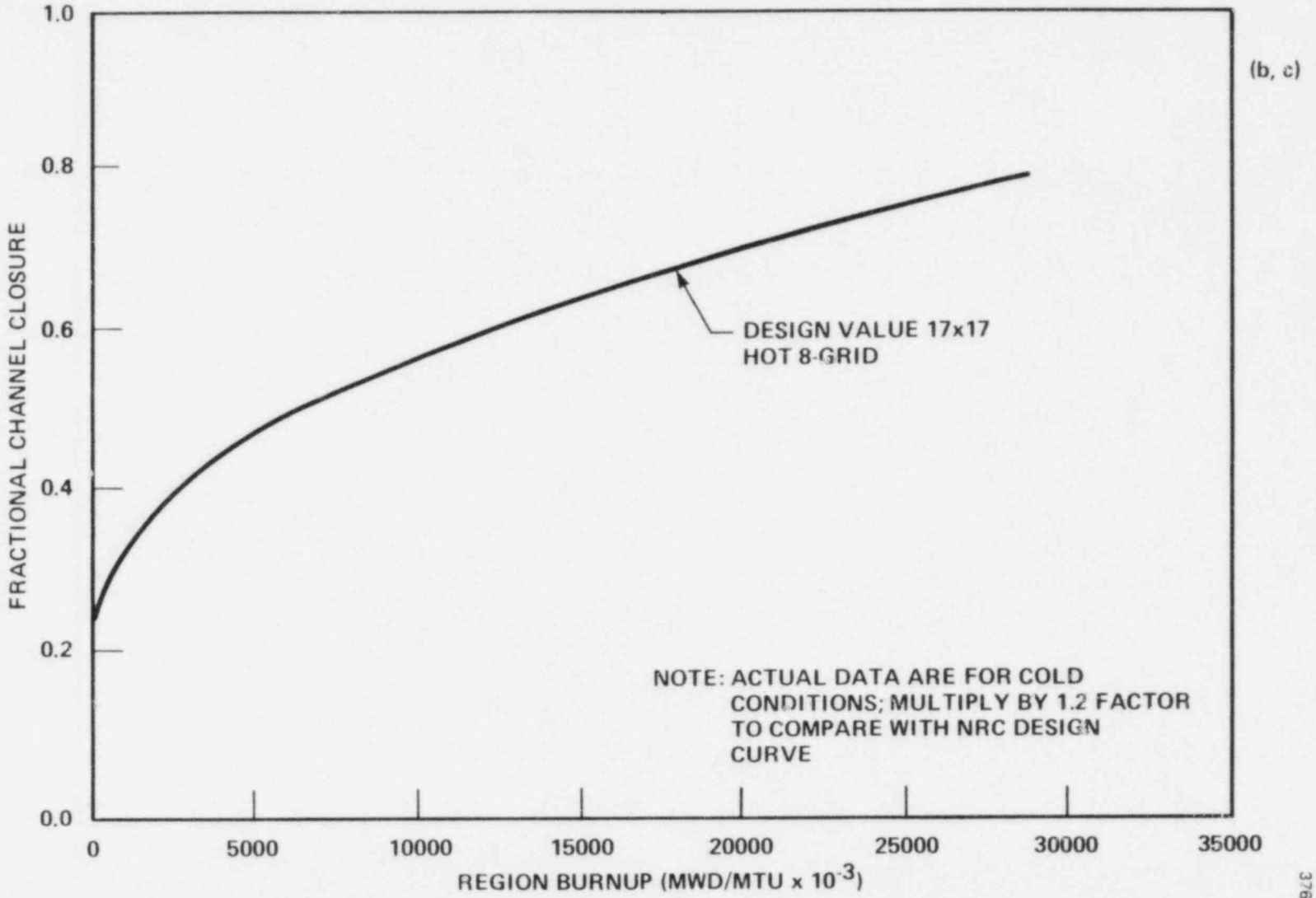

Figure 4-4. Worst-Span Channel Closure Behavior at the 95th Percentile Level

The low magnification television measurements of rod-to-nozzle gaps were calibrated for each fuel assembly face by measuring the television image of several grid springs (approximately the same length as the rod-to-nozzle gap) on the outside straps in the top grid and bottom grid on each assembly face. Measurements were taken from the television screen with drafting dividers and scaled from a machinist's ruler divided in 0.01-inch increments. The spring slot lengths on each top grid on each assembly face were averaged and used as a standard for determining the top nozzle-to-rod gaps on that face. Similarly, the spring slot lengths on each bottom grid were averaged and used as a standard for determining the bottom nozzle-to-rod gap on that face. The uncertainty in the calibration measurements and the rod-to-nozzle gap measurements was 5 percent.

The frequency distribution of total rod-to-nozzle gap (bottom plus top rod-to-nozzle gap) is shown in figure 4-5. The total rod-to-nozzle gap range from [ ] to [ ] inches with an average of [ ] inches for (b,c)
Region 2 assemblies and [ ] for Region 3 assemblies. Table 4-5 (b,c)
shows a summary of the average bottom gap, top gap, total gap and the maximum and minimum for the total gap. Figure 4-6 shows a typical example of face to face variations of top and bottom nozzle gaps in assembly B13. A decrease in the rod-to-nozzle gap at the top implies upward movement of the rod. A decrease in the gap at the bottom implies a downward movement of the rod. If the top gap remains uneffected, but the bottom gap decreases, rods are growing downwards. Slippage would be manifested as a decrease in the bottom gap and an increase in the top gap. The data generally show a downward growth, with substantial closure of bottom gap and little change in the top gap. This trend is consistent with data from other plants. Figure 4-6 shows that the bottom gaps on faces 1, 4 and 2 have changed slightly more from the nominal pre-irradiation value than the gaps of face 3. As shown in figure 3-3, face 3 of assembly B13 is located the farthest from the center of the core and will have the least burnup and since growth is burnup dependent, this observation is expected. One rod (rod 6) of face 2 of B13 was in contact with the bottom nozzle but it can be seen from figures 4-6 and 4-7 that the same rod has a larger top gap than the

3760

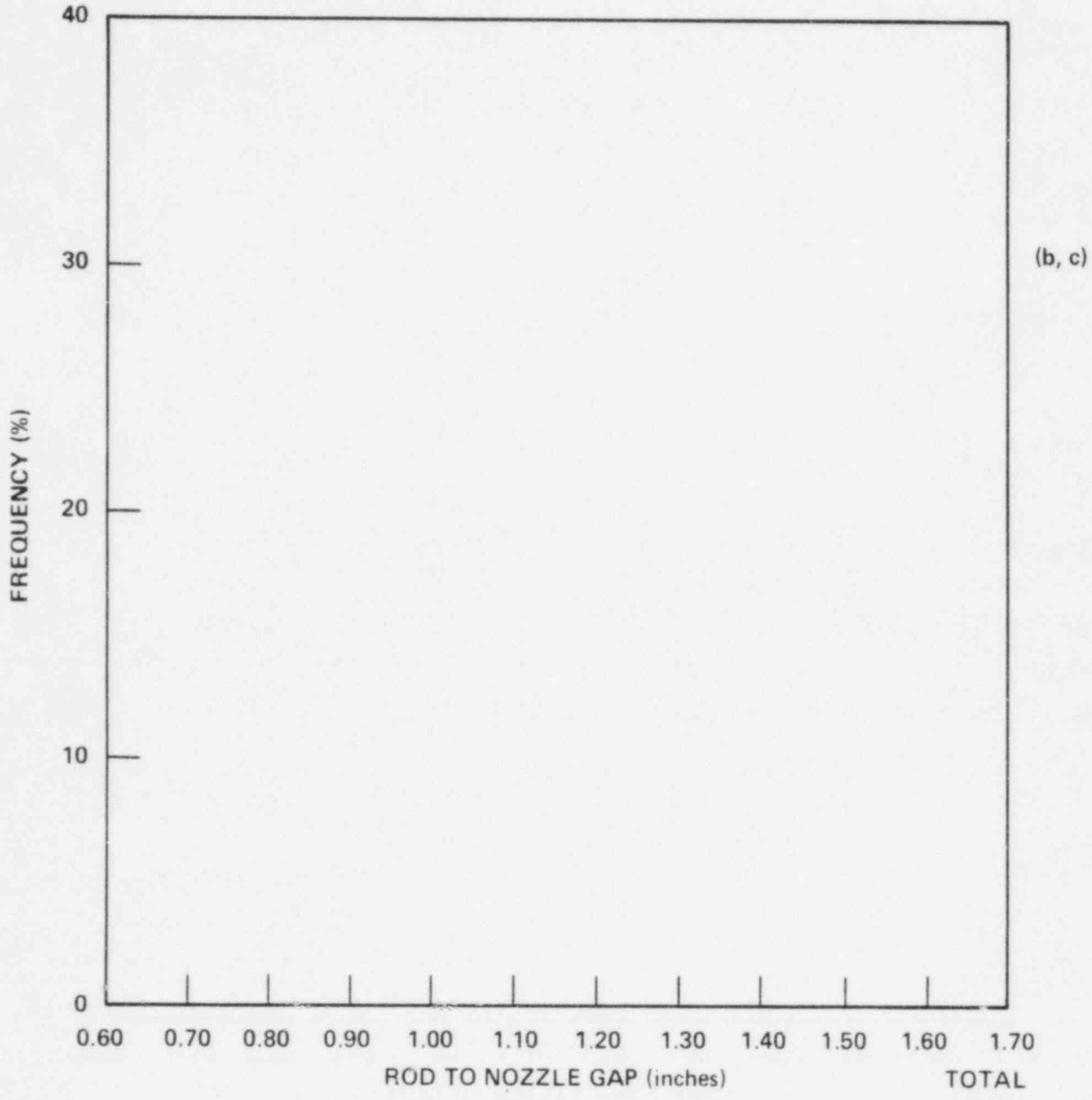

Figure 4-5. EOC-2 Distribution of Peripheral Fuel Rod to Nozzle Gaps (Bottom Gap Plus Top Gap) in Beaver Valley

3760

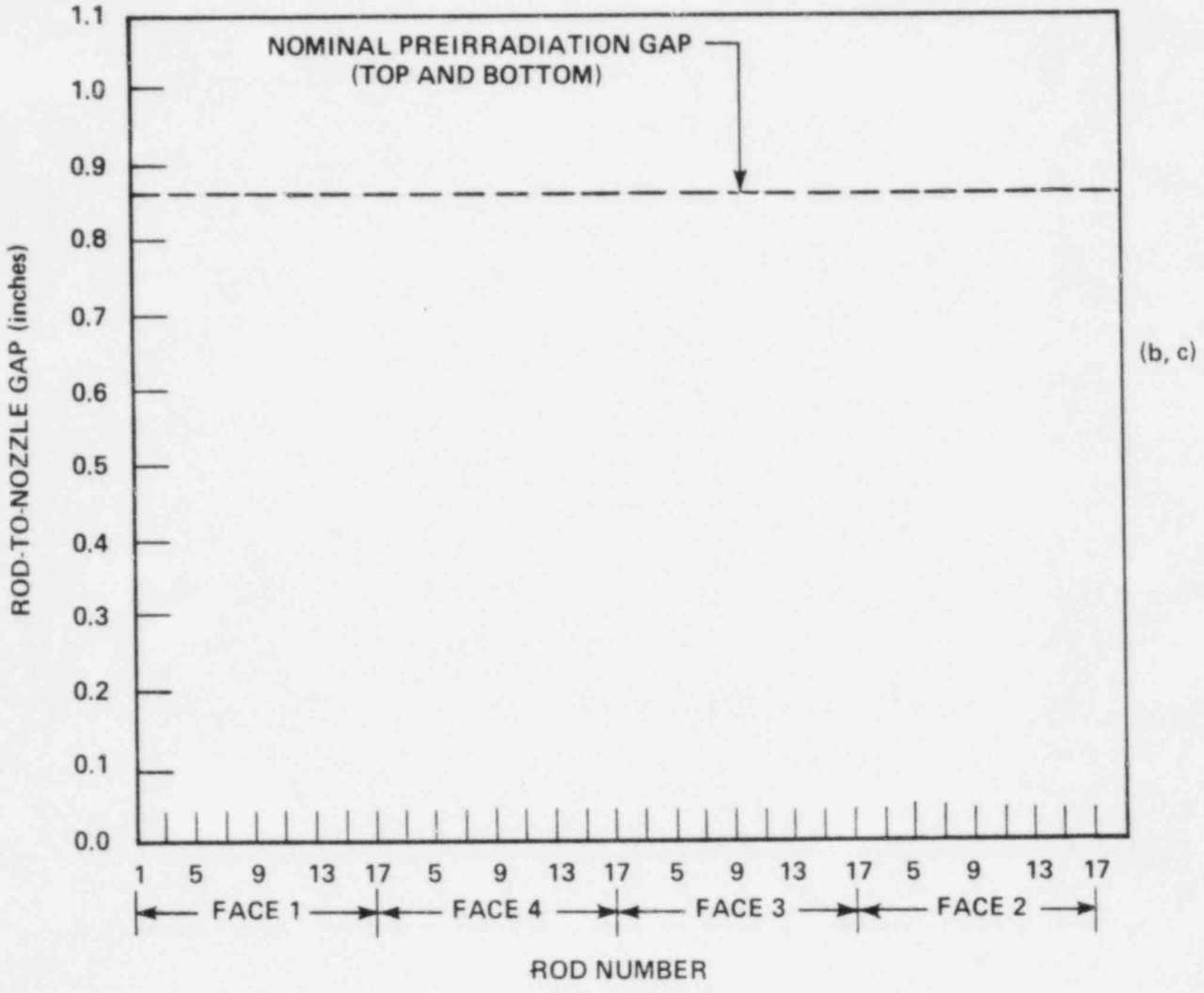

Figure 4-6. Face-to-Face Variation of Rod-to-Nozzle Gap in Fuel Assembly B13 After Two Cycles of Operation

nominal pre-irradiation value which indicates that there has been some downward slippage of the rod through the grid cell. The top gaps on the average for all faces of assembly B13 show a larger value than the nominal pre-irradiated value which is due primarily to a small amount of downward slippage of the rods.

One rod was observed to be in contact with the top nozzle, assembly B04, face 1, rod 3. Figure 4-8 shows the top and bottom gap for assembly B04 at the EOC-1 and EOC-2. The fact that the clearance between the rod and the bottom nozzle was also much larger than that of adjacent rods suggests that the rod has moved physically upward. As shown in figure 4-8, at the time when the visual examination was conducted at the EOC-1, rod 3 had the same axial position at the top as adjacent rods. The reason for the rod movement is not understood and is not consistent with prior 17x17 fuel examination experience.

Figure 4-7 shows typical rod-to-nozzle gaps at the EOC-1 and EOC-2. This figure shows that the bottom gap was substantially reduced at the higher burnup, while the top gap changed very little. Figures 4-9 and 4-10 respectively, show bottom gap change and top gap change data obtained for the nine assemblies as a function of region average burnup, and compare with data from several other plants is also illustrated. These figures indicate that the gap changes observed in Beaver Valley are consistent with the gap changes seen in other plants. As shown in figures 4-7 and 4-9, the bottom gap decreases continuously with burnup. However, the top gap changes little with burnup. This observation implies that fuel rods tend to grow predominantly downward until the bottom gap is fully closed, although occasionally fuel rods slip slightly downward through the grids. The gap data obtained for Beaver Valley assemblies indicate than an adequate rod-to-nozzle gap exists to accommodate continued rod growth for further cycles of irradiation.

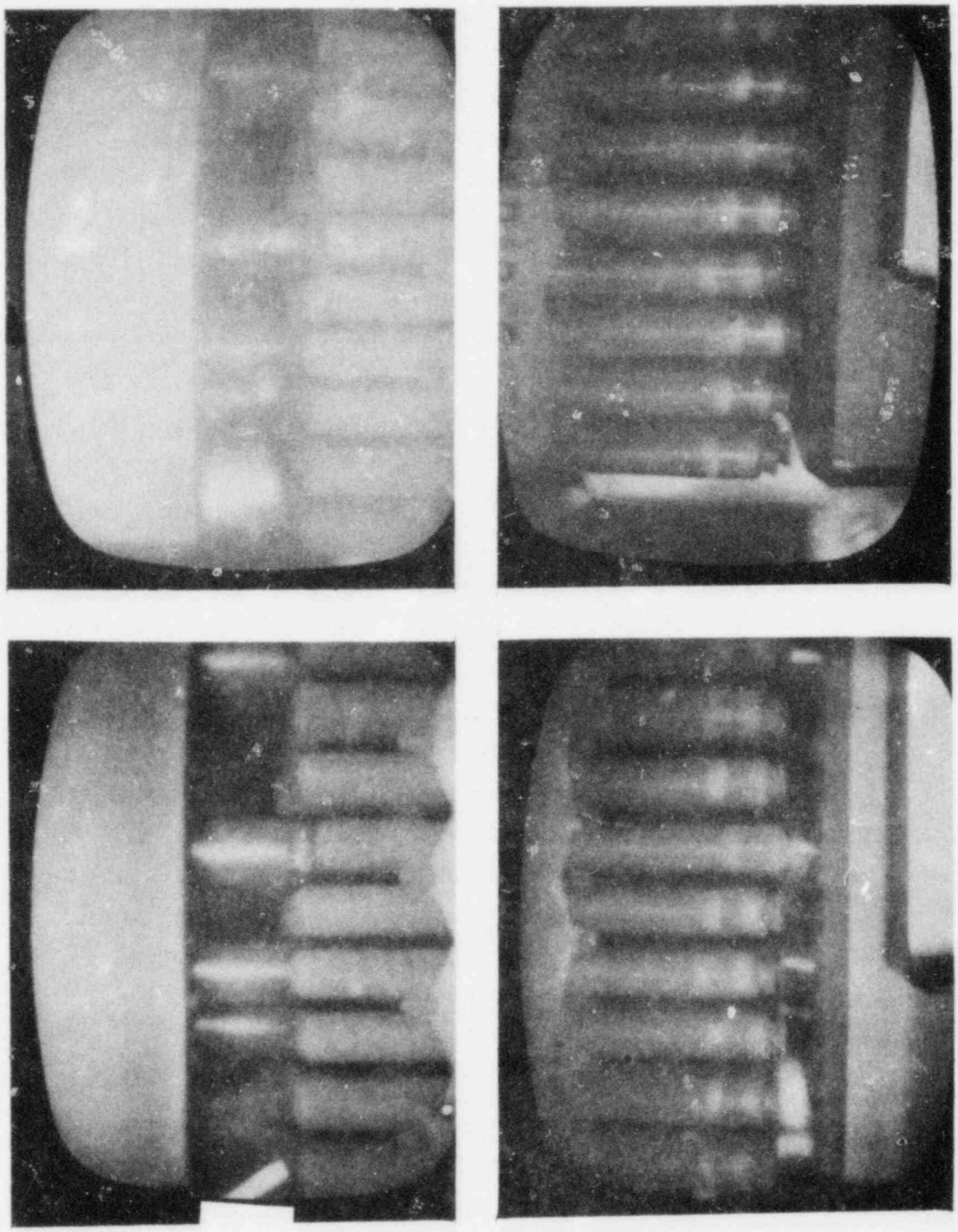

Figure 4-7 Typical Rod-to-Nozzle Gaps at EOC-1 and EOC-2 (Assembly B13, Face 2, Left side)

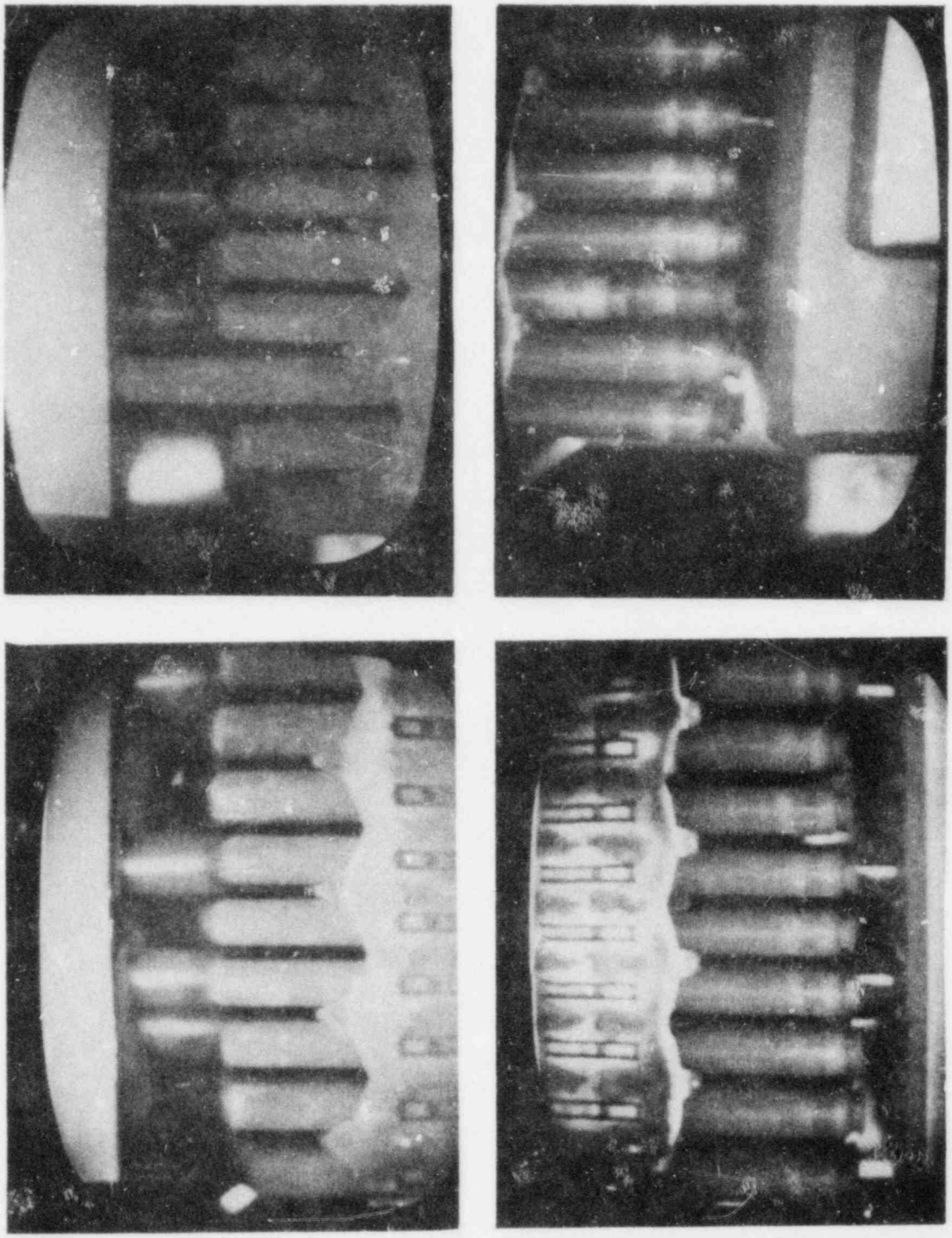

Figure 4-8 Top and Bottom Gap of Assembly B04 Left Side Face 1, EOC-1 and 2

Fuel rod growth for each rod examined was derived from the rod-to nozzle gap data and the predicted fuel assembly growth based upon data from other sites.

Fuel rod growth was derived from the gap measurements using the equation:

$$\text{Rod Growth} = 100 \times \frac{[\ A+B-C\ ]}{D}$$

A = Preirradiation nominal total gap

B = Irradiation change in nozzle-to-nozzle length (nominal preirradiation nozzle-to-nozzle length times the EOC-2 assembly growth)
Nominal preirradiated nozzle-to-nozzle length = [ ] (a,c)

C = EOC-2 rod-to-nozzle gap

D = Preirradiation nominal rod length = [ ] (a,c)

Fuel rod growth after 2 cycles, summarized in Table 4-5 range from [ ] (b,c) to [ ] percent with a mean of [ ] percent for Region 2 and [ ] (b,c) percent for Region 3.

Figure 4-11 plots the combined rod growth data for the nine Beaver Valley assemblies as a function of fast fluence, together with data from several other plants. The Beaver Valley rod growth data are consistent with the data obtained from other plants.

Figure 4-11 shows that there is a large degree of variability in rod growth among the peripheral rods, probably resulting from varying

TABLE 4-5

BEAVER VALLEY EOC-2
ROD-TO-NOZZLE GAP AND ROD GROWTH

FUEL ASSEMBLY NUMBER	BURNUP	AVERAGE (IN) BGAP	TGAP	TOTGAP	TOT GAP MAX	MIN	PERCENT ROD GROWTH	PERCENT ROD GROWTH MAX	MIN
B04									
B07									
B13									
B20									
B31									
C03									
C06									
C15									
C39									
AVERAGE REGION B									
AVERAGE REGION C									

(b,c)

3760

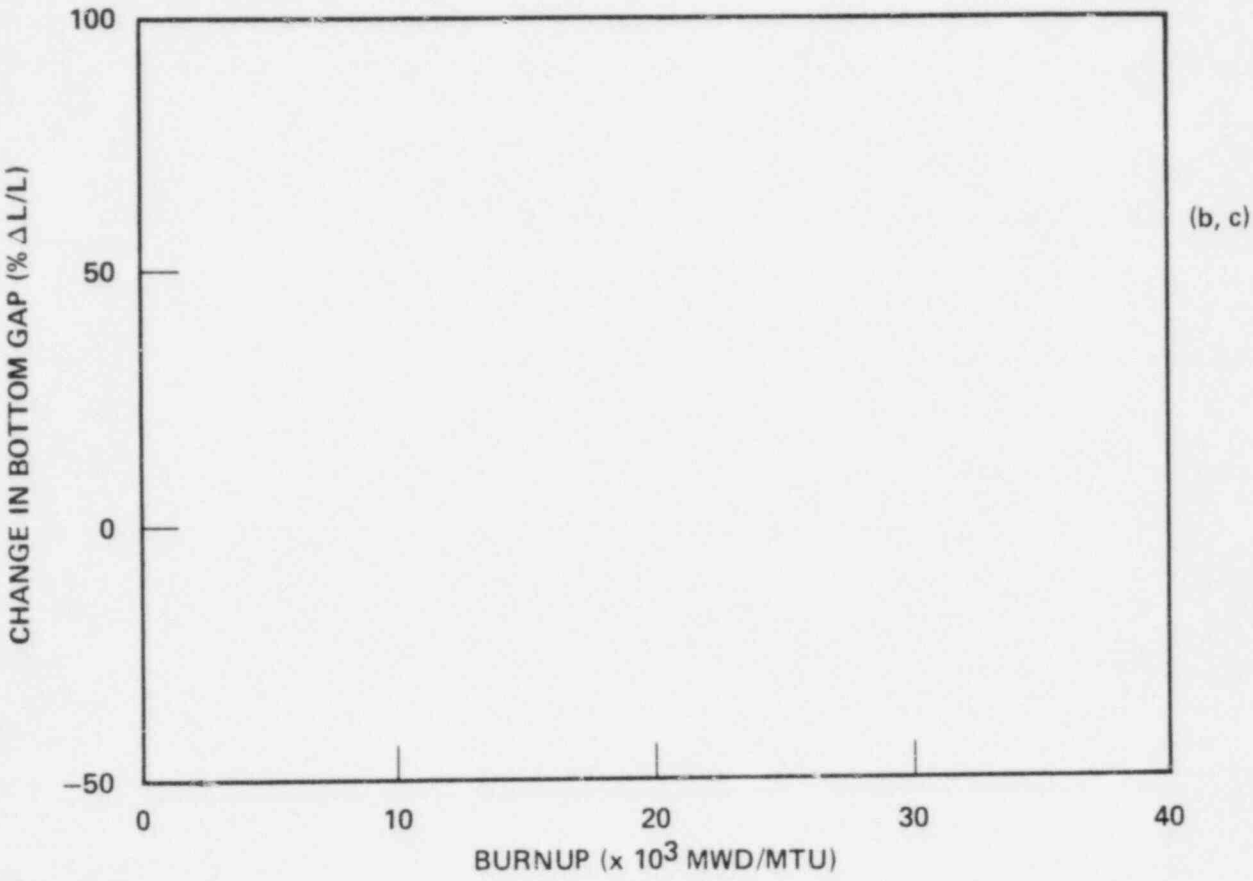

Figure 4-9. Bottom Gap Change Versus Burnup

3760

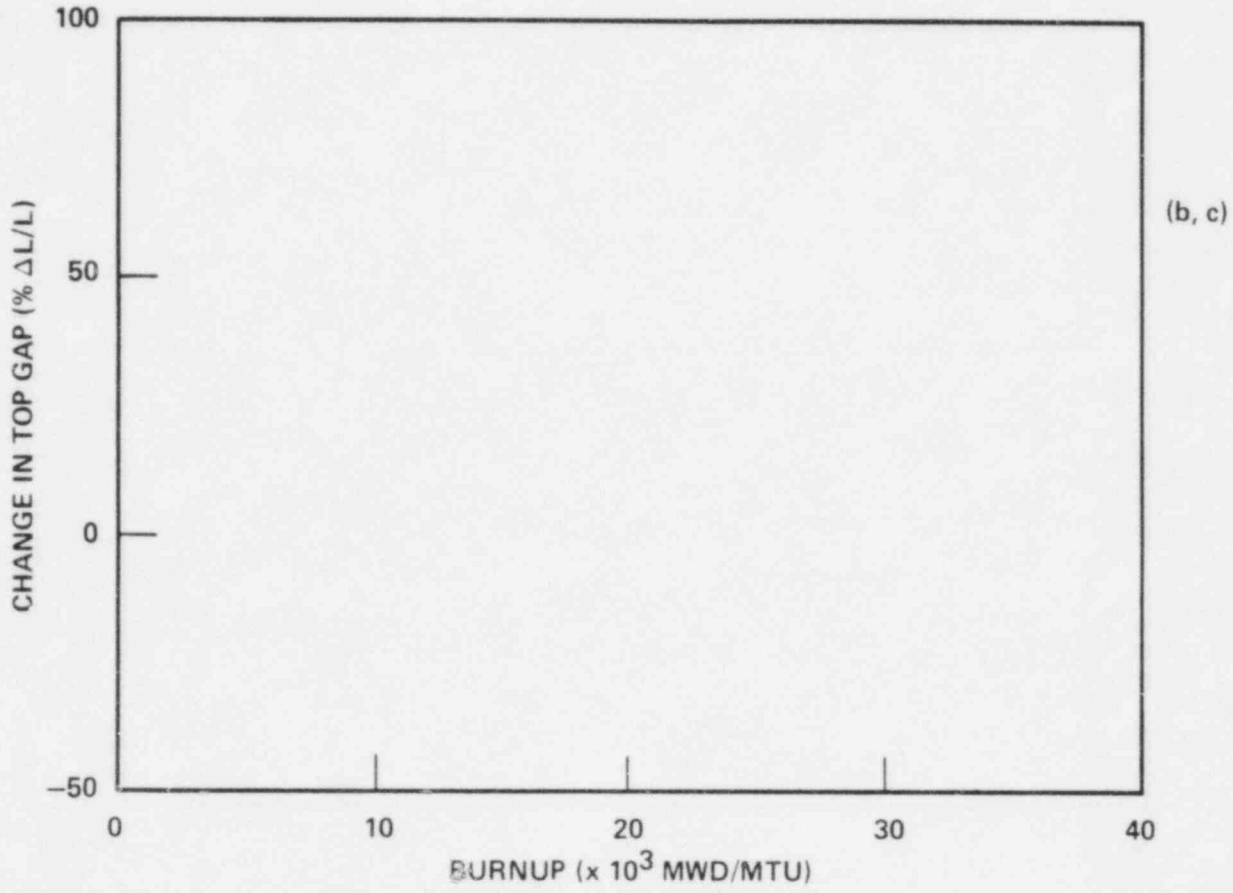

Figure 4-10. Top Gap Change Versus Burnup

3760

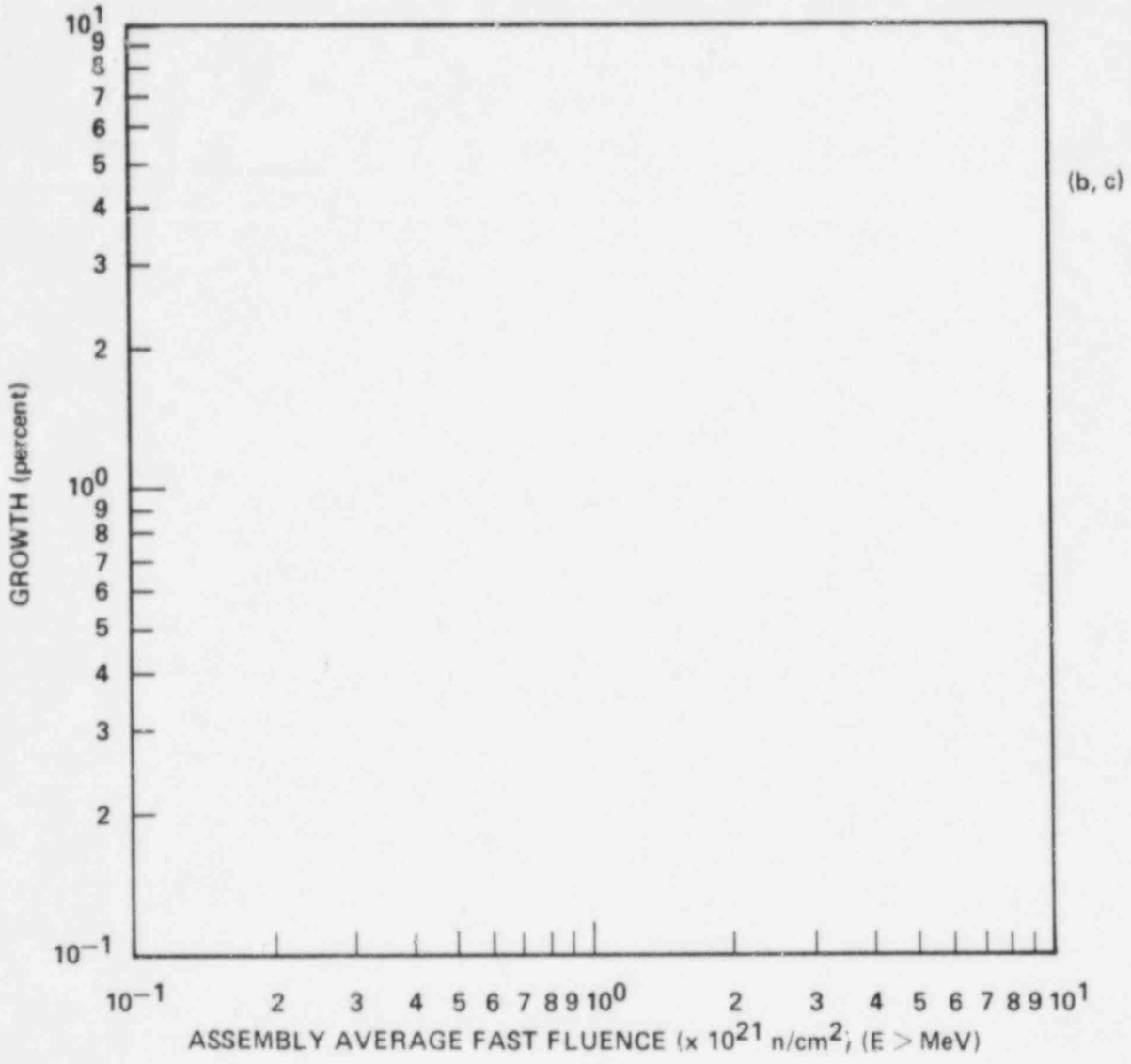

Figure 4-11. Fuel Rod Growth Variation with Fluence

fluences, slight difference in metallurgical conditions of the tubing, and varying amounts of stress components from rod to rod. Irradiation growth studies have shown that the free growth components increases with fast fluence and is strongly dependent on cladding texture, degree of cold work, and heat treatment. Additionally, Zircaloy growth is influenced by stress components which act on the Zircaloy structure, due to externally applied grid forces and internally applied fuel pellet forces.

4.2.4 EXAMINATION OF FUEL ASSEMBLIES AT BAFFLE JOINT

Recent fuel inspections at several reactors reveal that when coolant cross flow through leaking baffle joints impinges against peripheral fuel rods, fuel rod vibration and resultant fretting wear in the grids may occur. Since Beaver Valley has similar baffle joint geometries (center injection joints) to plants where damage has been observed, assemblies in Beaver Valley adjacent to these joint types were examined. Twenty fuel assemblies were inspected to determine the condition of the fuel rods and of corresponding grid cells located adjacent to the baffle joints. The core locations of these assemblies are shown in figure 4-12. The examinations were performed on seven rods on the face of the assembly directly adjacent to the center injection baffle joint using two high magnification scans with four rods per scan (one rod overlap); Table 4-6 lists the assemblies, faces, and fuel rods that were examined.

None of the rods in the 20 region 4 fuel assemblies examined showed obvious baffle joint flow induced rod damage such as open defects, cracks, axial clad splits, worn clad flats, or detectable channel spacing reduction at grids. However, T.V. visual examinations indicated that several assemblies exhibited clean white marks on the grids. Thus an indication of minor baffle joint flow. The assemblies, faces, grids and rod locations exhibiting the marks are summarized in Table 4-7. A typical example of the clean white mark is shown in figure 4-13. In

addition to this evidence of minor jetting, other characteristics of jetting from flow were noted. Rod 12 on face 3 of assembly D36 exhibited about 1/4 inch downward slippage as shown in figure 4-14. This is believed to be due to excessive vibration and grid cell relaxation. Three assemblies D38, D24 and D09 exhibited rod bow due to the Bernoulli effect. The rod bow was caused by Bernoulli forces generated due to pressure difference around the rods due to crossflow through the baffle joint. Bernoulli rod bow occurred directly opposite the jet in the lower grid spans. Figure 4-15a illustrates the mechanism of the Bernoulli effect. Figure 4-15 shows an instance of Bernoulli bow for fuel assembly D24. Another indication of baffle joint flow was a clean darker clad surface along the rod generally seen on rod number 3 counted from the assembly corner closest to the center injection baffle joint.

None of the assemblies exhibited evidence of fuel rod failure, or damage due to baffle jetting sufficient to prevent the fuel assemblies from being reloaded for continued irradiation.

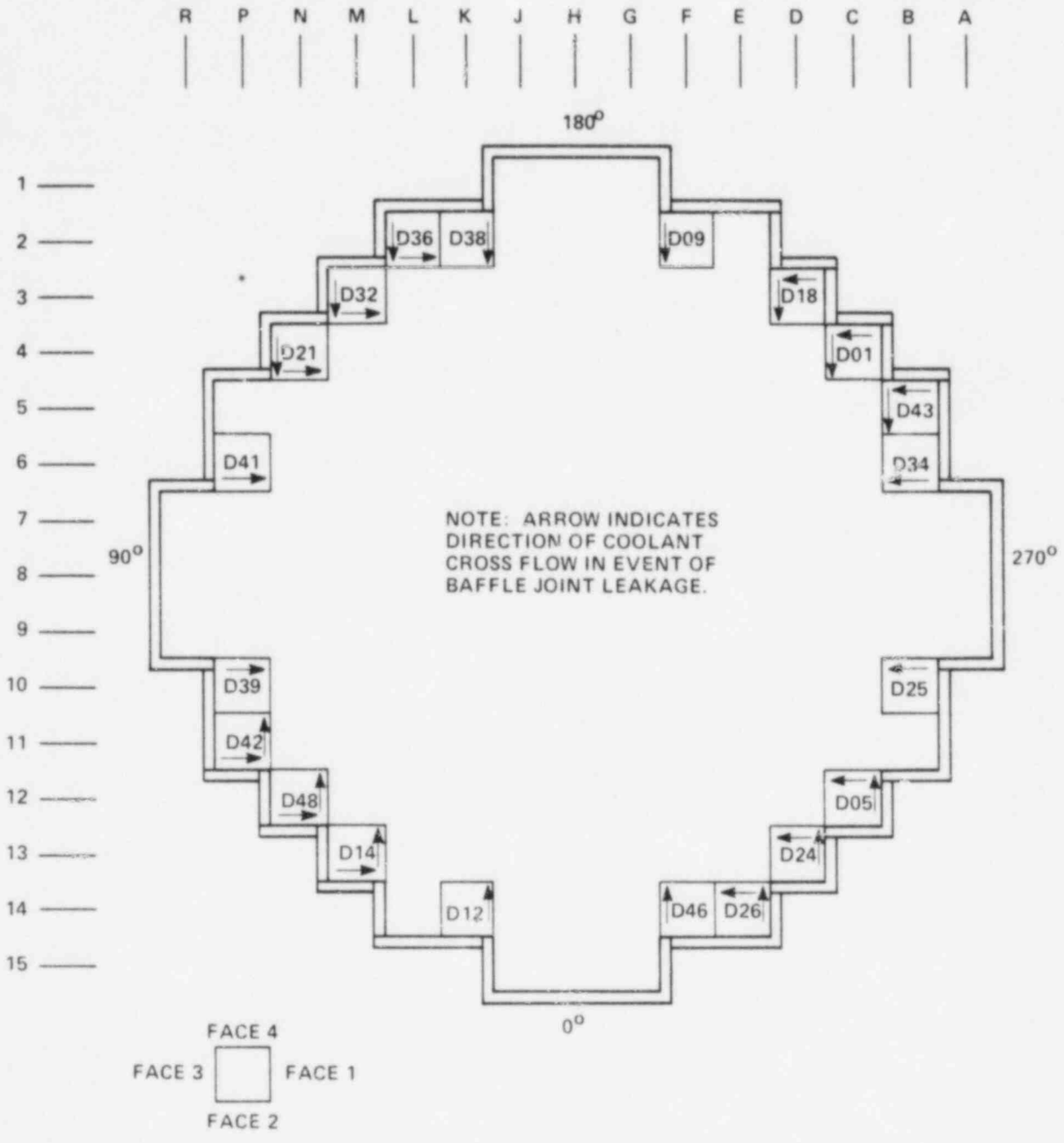

Figure 4-12. Location of Fuel Assemblies Examined for Effects of Coolant Cross Flow Through Baffle Joints

TABLE 4-6

BEAVER VALLEY EOC-2 HIGH MAG T.V. VISUALS OF BAFFLE ASSEMBLIES

Assembly Number	Core Position	Face	Rods
D09	F01	3	1-8
		4	10-17
D46	F14	2	1-8
		3	10-17
D26	E14	1	10-17
		4	1-8
D36	L02	3	10-17
		2	1-8
D32	M03	3	10-17
		2	1-8
D24	D13	1	11-17
		4	1-7
D14	M13	1	1-7
		2	11-17
D18	D03	3	1-7
		4	11-17
D38	K02	1	11-17
		4	1-7
D12	K14	1	1-7
		2	11-17
D41	P06	2	1-7
		3	11-17
D34	B06	1	1-7
		2	11-17
D21	N04	2	1-7
		3	11-17
D48	N12	1	1-7
		2	11-17
D01	C04	3	1-7
		4	11-17
D05	C12	1	11-17
		4	1-7

TABLE 4-6 (Cont'd)

BEAVER VALLEY EOC-2 HIGH MAG T.V. VISUALS OF BAFFLE ASSEMBLIES

Assembly Number	Core Position	Face	Rods
D43	B05	3	1-7
		4	11-17
D42	P11	1	1-7
		2	11-17
D25	B10	1	11-17
		4	1-7
D39	P10	3	1-7
		4	11-17

TABLE 4-7

ASSEMBLIES EXHIBITING CLEAN WHITE MARK ON GRIDS

Assemblies No.	Face No.	Grid No.*	Rod Location**
D41	3	4,5,6	between rods 2 and 3
D34	1	5,6	"
D38	4	4,5,6	"
D32	3	3,4,5,6	"
D46	2	3,4,5	"
D25	1	4,5,6	"

*Grid location counted from the bottom of the assembly.

**Rod counted from the assembly corner closest to the center injection baffle joint.

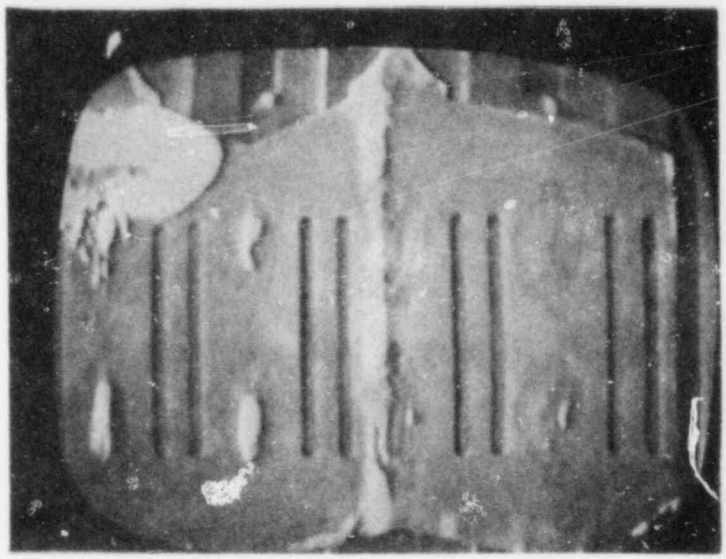

Figure 4-13 Example of White
Clean Mark on Grid 6 on
Face 3 of Assembly D41

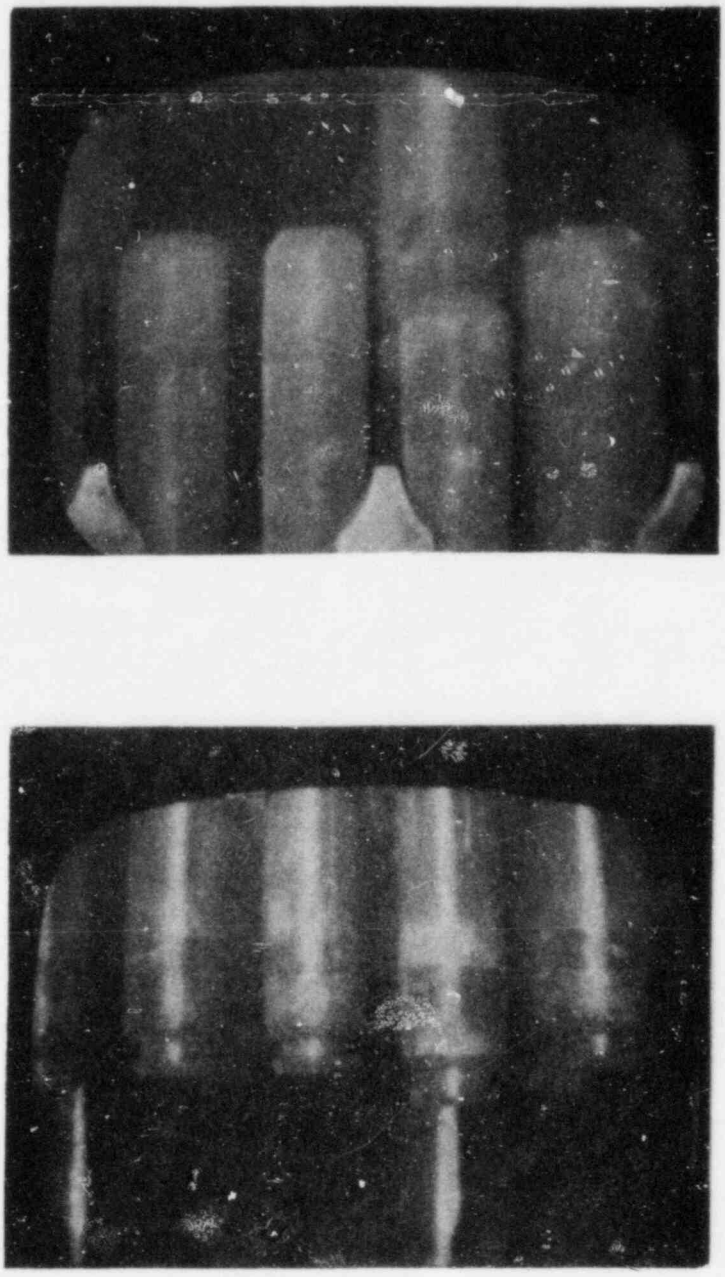

Figure 4-14 Assembly D36 Face 3 (Rod 12 Exhibits Downward Slippage)

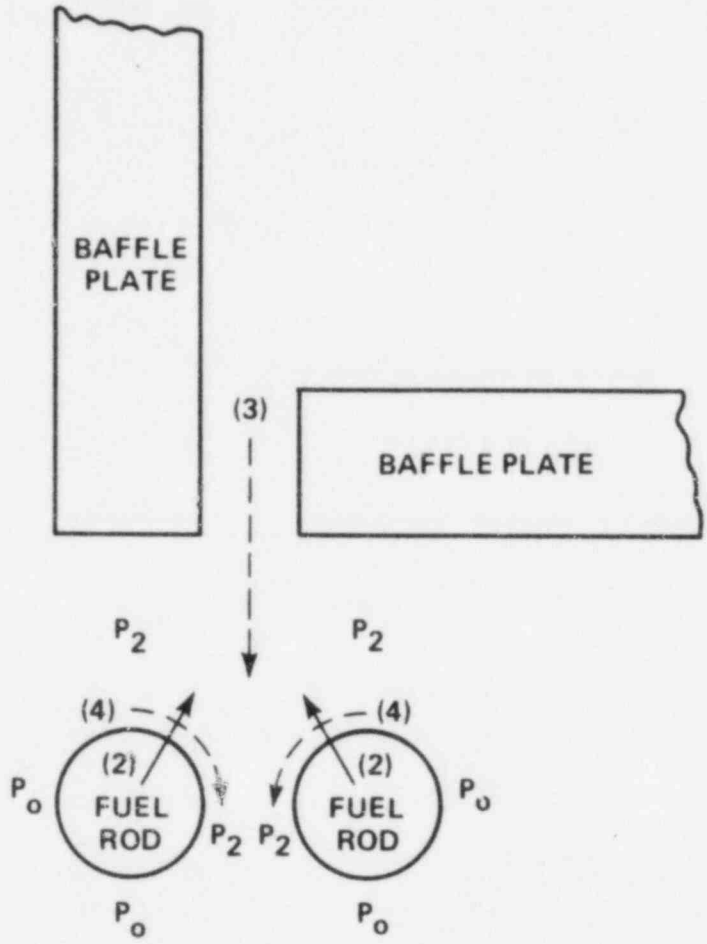

(1) P_o: COOLANT PRESSURE

P_2: COOLANT PRESSURE

$P_o > P_2$

(2) BERNOULLI FORCE WORKED ON ROD

(3) BAFFLE JETTING CROSS FLOW

(4) CROSS FLOW AROUND ROD GENERATED BY BAFFLE JETTING FLOW

Figure 4-15A. Illustration of Mechanism of Channel Closure Due to Bernoulli Effect

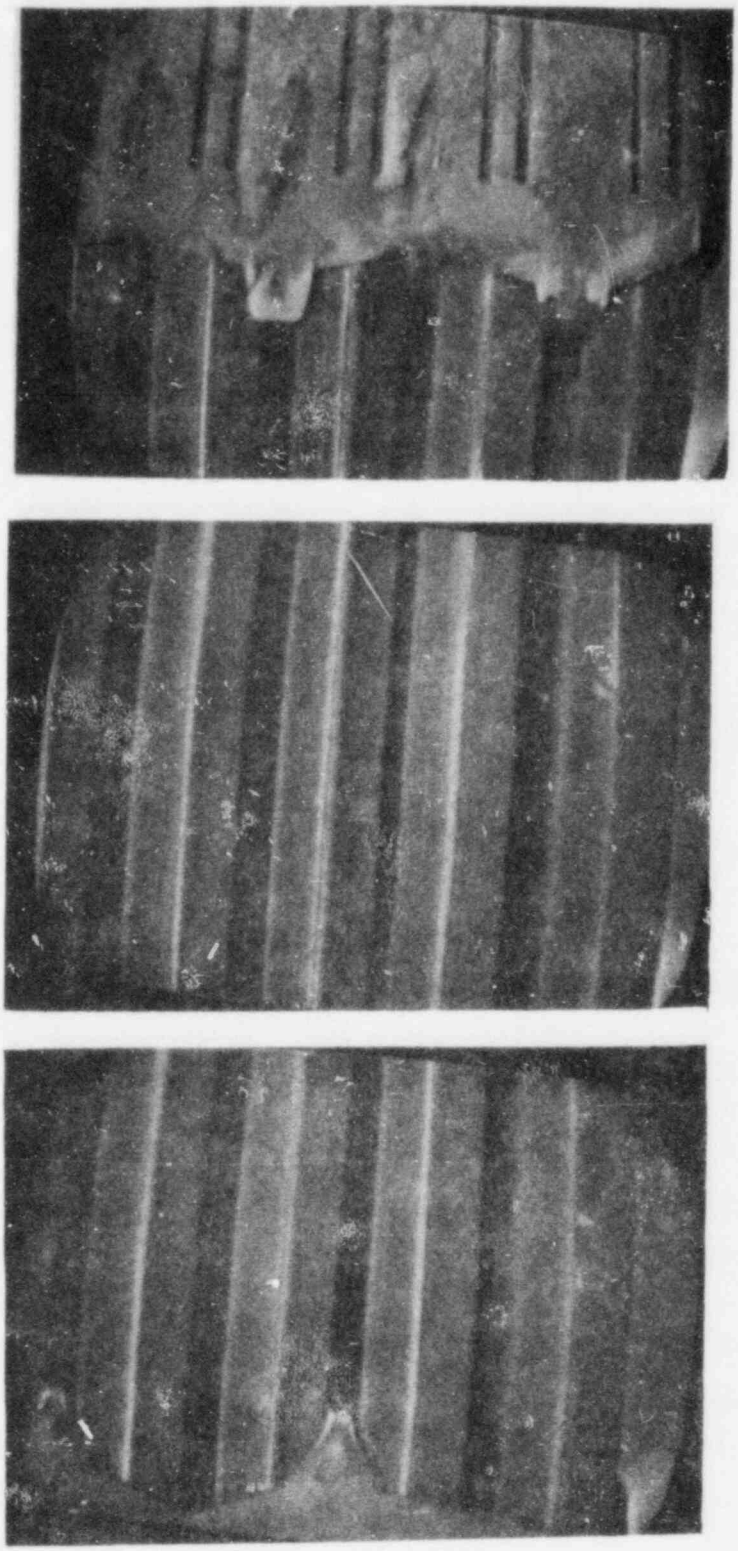

Figure 4-15 Detectable Reduction in Channel Between Rods 15 and 16 at Midspan Between Grids 1 and 2 on Face 1 of Assembly D24

SECTION 5

CONCLUSIONS

The examination of a representative sample of Beaver Valley Unit 1 fuel assemblies after two cycles of operation showed the assemblies to be in excellent condition. Crud deposits were moderate, there was no evidence of thick crud of the type which could cause concern for excessive cladding corrosion.

Less than [ ] percent of the peripheral fuel rod channels in 10 assemblies examined were closed [ ] percent or more due to rod bow. (b,c) (b,c)
The 95th percentile worst-span rod bow is consistent with other 17x17 data and well within the NRC design limit. Rod growth was observed to be consistent with other 17x17 data; ample fuel rod-to-nozzle gap exists for continued irradiation without risk of interference. Examination of 20 assemblies adjacent to center injection baffle joints showed no gross baffle joint flow induced rod damage such as open defects, cracks, worn clad flats or detectable channel spacing reduction at the grids. However, evidence of minor jetting at the joints was noted.

SECTION 6

REFERENCES

1. W. G. Kotsenas, J. B. Melehan, First Cycle Performance of Beaver Valley Unit 1 Fuel, WCAP-9731, August, 1980. (Westingnouse Proprietary)

2. P. H. Huang, L. A. Klotz, The Nuclear Design and Core Management of the Beaver Valley Unit 1 Power Plant Cycle 3, WCAP-10037, February, 1982. (Westinghouse Proprietary)

3. Solomon Y., and J. Roesmer, Some Observations on the Possible Relationship of Reactor Coolant Chemistry and Radiation Level Buildup, WCAP-9407, November, 1978.

4. Sweeton, F. H. and C. F. Baes Jr., The Solubility of Magnetite and Hydrolysis of Ferrous Ion in Aqueous Solutions at Elevated Temperatures, J. Chem Thermodyn 2, pp 479-500 (1970).

5. H. Kunishi, Second Cycle Performance of Salem Unit 1 Fuel, WCAP-9874, May, 1981. (Westinghouse Proprietary)

6. J. B. Melehan, et al., Trojan Cycle 3 Fuel Performance, WCAP-9963, December, 1981. (Westinghouse Proprietary)

7. DeStefano, J. et al., Interim Report Surry Unit 1 EOC-3 Onsite Fuel Examination of 17x17 Demonstration Assemblies after Two Cycles of Exposure, WCAP-9139, June, 1978.

8. Schmidt, G. R., et al., Interim Report Surry Unit 2 EOC-3 Fuel Examination of 17x17 Demonstration Assemblies after Two Cycles of Exposure, WCAP-9238, January, 1979.

APPENDIX A

SUMMARY OF PERIPHERAL ROD CHANNEL CLOSURES IN BEAVER VALLEY UNIT 1 FUEL ASSEMBLIES

Fuel Assembly	Span	Number of Channel Closures in Magnitude Ranges
B04	7	
	6	(b,c)
	5	
(EOC-1)	4	
	3	
	2	
	1	

Fuel Assembly	Span	Number of Channel Closures in Magnitude Ranges
B04	7	
	6	
	5	(b,c)
(EOC-2)	4	
	3	
	2	
	1	

Fuel Assembly	Span	Number of Channel Closures in Magnitude Ranges
B07	7	
	6	(b,c)
	5	
(EOC-1)	4	
	3	
	2	
	1	

Fuel Assembly	Span	Number of Channel Closures in Magnitude Ranges
B07	7	
	6	
	5	(b,c)
(EOC-2)	4	
	3	
	2	
	1	

Fuel Assembly	Span	Number of Channel Closures in Magnitude Ranges
B13	7	
	6	(b,c)
	5	
(EOC-1)	4	
	3	
	2	
	1	

Fuel Assembly	Span	Number of Channel Closures in Magnitude Ranges
B13	7	
	6	(b,c)
	5	
(EOC-2)	4	
	3	
	2	
	1	

Fuel Assembly	Span	Number of Channel Closures in Magnitude Ranges
B20	7	(b,c)
	6	
	5	
(EOC-1)	4	
	3	
	2	
	1	

Fuel Assembly	Span	Number of Channel Closures in Magnitude Ranges
B20	7	(b,c)
	6	
	5	
(EOC-2)	4	
	3	
	2	
	1	

Fuel Assembly	Span	Number of Channel Closures in Magnitude Ranges	
B31	7		
	6		(b,c)
	5		
(EOC-1)	4		
	3		
	2		
	1		

Fuel Assembly	Span	Number of Channel Closures in Magnitude Ranges	
B31	7		
	6		(b,c)
	5		
(EOC-2)	4		
	3		
	2		
	1		

Fuel Assembly	Span	Number of Channel Closures in Magnitude Ranges	
C03	7		(b,c)
	6		
	5		
(EOC-1)	4		
	3		
	2		
	1		

Fuel Assembly	Span	Number of Channel Closures in Magnitude Ranges	
C03	7		
	6		
	5		(b,c)
(EOC-2)	4		
	3		
	2		
	1		

Fuel Assembly	Span	Number of Channel Closures in Magnitude Ranges
C06	7	
	6	(b,c)
	5	
(EOC-1)	4	
	3	
	2	
	1	

Fuel Assembly	Span	Number of Channel Closures in Magnitude Ranges
C06	7	
	6	
	5	(b,c)
(EOC-2)	4	
	3	
	2	
	1	

Fuel Assembly	Span	Number of Channel Closures in Magnitude Ranges
C15	7	
	6	(b,c)
	5	
(EOC-1)	4	
	3	
	2	
	1	

Fuel Assembly	Span	Number of Channel Closures in Magnitude Ranges
C15	7	
	6	
	5	(b,c)
(EOC-2)	4	
	3	
	2	
	1	

Fuel Assembly	Span	Number of Channel Closures in Magnitude Ranges
C39	7	
	6	(b,c)
	5	
(EOC-1)	4	
	3	
	2	
	1	

Fuel Assembly	Span	Number of Channel Closures in Magnitude Ranges
C39	7	
	6	
	5	(b,c)
(EOC-2)	4	
	3	
	2	
	1	

Fuel Assembly	Span	Number of Channel Closures in Magnitude Ranges	
C49	7		
	6		(b,c)
	5		
(EOC-1)	4		
	3		
	2		
	1		

Fuel Assembly	Span	Number of Channel Closures in Magnitude Ranges	
C49	7		
	6		(b,c)
	5		
(EOC-2)	4		
	3		
	2		
	1		